



2018-04-01

Chloride Concentration and Blow-Through Analysis for Concrete Bridge Decks Rehabilitated Using Hydro-Demolition

Elizabeth Ashleigh Roper
Brigham Young University

Follow this and additional works at: <https://scholarsarchive.byu.edu/etd>



Part of the [Civil and Environmental Engineering Commons](#)

BYU ScholarsArchive Citation

Roper, Elizabeth Ashleigh, "Chloride Concentration and Blow-Through Analysis for Concrete Bridge Decks Rehabilitated Using Hydro-Demolition" (2018). *All Theses and Dissertations*. 6779.
<https://scholarsarchive.byu.edu/etd/6779>

This Thesis is brought to you for free and open access by BYU ScholarsArchive. It has been accepted for inclusion in All Theses and Dissertations by an authorized administrator of BYU ScholarsArchive. For more information, please contact scholarsarchive@byu.edu, ellen_amatangelo@byu.edu.

Chloride Concentration and Blow-Through Analyses for Concrete
Bridge Decks Rehabilitated Using Hydrodemolition

Elizabeth Ashleigh Roper

A thesis submitted to the faculty of
Brigham Young University
in partial fulfillment of the requirements for the degree of
Master of Science

W. Spencer Guthrie, Chair
Fernando S. Fonseca
Kevin W. Franke

Department of Civil and Environmental Engineering
Brigham Young University

Copyright © 2018 Elizabeth Ashleigh Roper

All Rights Reserved

ABSTRACT

Chloride Concentration and Blow-Through Analyses for Concrete Bridge Decks Rehabilitated Using Hydrodemolition

Elizabeth Ashleigh Roper

Department of Civil and Environmental Engineering, BYU
Master of Science

The objectives of this research were 1) to investigate the effects of hydrodemolition treatment timing on chloride concentration profiles in concrete bridge decks for depths of concrete removal below the top mat of reinforcing steel and 2) to investigate factors that influence the occurrence of blow-throughs in concrete bridge decks when hydrodemolition is used. The research results are intended to provide engineers with guidance about the latest timing of hydrodemolition that can maintain a chloride concentration level below 2.0 lb of chloride per cubic yard of concrete at the levels of both the top and bottom mats of reinforcing steel, as well as about conditions that may indicate a higher probability of blow-through during hydrodemolition. The scope of this research included a questionnaire survey of hydrodemolition companies to summarize common practices in the field, numerical modeling of chloride concentration to investigate hydrodemolition treatment timing on typical Utah bridge decks, and structural analysis to investigate factors that influence the occurrence of blow-throughs during hydrodemolition.

While some survey respondents indicated that certain parameters vary, the responses are valuable for understanding typical practices and were used to design the numerical experiments. The numerical modeling generated chloride concentration profiles through a 75-year service life given a specific original cover depth (OCD), treatment time, and surface treatment usage. The results indicate that, when a surface treatment is used, the concentration at either the top or bottom mat of reinforcing steel does not reach or exceed 2.0 lb of chloride per cubic yard of concrete after hydrodemolition during the 75 years of simulated bridge deck service life. The results also indicate that, when a surface treatment is not used, the chloride concentration at the top mat of reinforcement exceeds 2.0 lb of chloride per cubic yard of concrete within 10, 15, and 20 years for OCD values of 2.0, 2.5, and 3.0 in., respectively. The numerical experiments generated results in terms of the main effect of each input variable on the occurrence of blow-throughs and interactions among selected input variables. For each analysis, blow-through can be expected when the calculated factor of safety is less than 1.0. The factor of safety significantly increases with increasing values of transverse rebar spacing and concrete compressive strength and decreasing values of depth of removal below the bottom of the top reinforcing mat, orifice size, and water pressure within the ranges of these parameters investigated in this experimentation. The factor of safety is relatively insensitive to jet angle. For both case studies evaluated in this research, the blow-through analysis correctly predicted a high or low potential for blow-through on the given deck.

Key words: blow-through, chloride concentration, concrete bridge deck, diffusion, hydrodemolition, surface treatment

ACKNOWLEDGEMENTS

The Utah Department of Transportation (UDOT) and the Brigham Young University (BYU) Office of Research and Creative Activities provided funding for this research. The National Institute of Standards and Technology provided the software program used for numerical modeling of chloride concentration, and John De Leon, a member of the BYU Materials and Pavements Research Group, initiated creation of the spreadsheet used for blow-through analysis. Information about current bridge deck rehabilitation practices was obtained from UDOT and several hydrodemolition companies, including HydroPressure Cleaning, Inc.; Hydro-Technologies, Inc.; Midwest Mobile Waterjet; Rampart Hydro Services, L.P.; and Redi Services, LLC. I appreciate the support, guidance, and mentorship of Dr. Fernando S. Fonseca and Dr. Kevin W. Franke as members of my graduate advisory committee. I am especially grateful for the time, care, and mentorship that Dr. W. Spencer Guthrie has given me through my most difficult academic years; he has taught me by example the importance of integrity, respect, and hard work. I am grateful to my parents, Greg and Tammara Newbill, who have always encouraged me to work hard in order to reach my most important goals. Finally, I thank my husband, Aaron, who has supported and encouraged me as I accomplished my academic and occupational goals.

TABLE OF CONTENTS

LIST OF TABLES.....	vi
LIST OF FIGURES	vii
1 INTRODUCTION	1
1.1 Problem Statement	1
1.2 Research Objectives and Scope.....	5
1.3 Outline of Report.....	5
2 BACKGROUND	7
2.1 Overview.....	7
2.2 Chloride-Induced Corrosion of Reinforcing Steel.....	7
2.3 Removal of Deteriorated Concrete Using Hydrodemolition	9
2.4 Application of Surface Treatments to Concrete Bridge Decks.....	12
2.5 Summary	13
3 EXPERIMENTAL METHODOLOGY	15
3.1 Overview.....	15
3.2 Questionnaire Survey.....	15
3.3 Chloride Concentration Analysis	16
3.4 Blow-through Analysis	22
3.5 Summary	30
4 RESULTS AND ANALYSIS.....	33
4.1 Overview.....	33
4.2 Questionnaire Survey.....	33
4.3 Chloride Concentration Analysis	36
4.4 Blow-through Analysis	42
4.5 Summary	58
5 CONCLUSION.....	61
5.1 Summary	61
5.2 Findings.....	63
5.3 Recommendations.....	65

REFERENCES	67
APPENDIX A SAMPLE INPUTS FOR CHLORIDE CONCENTRATION ANALYSIS.....	70
APPENDIX B BLOW-THROUGH ANALYSIS FOR CASE STUDY #1	76
APPENDIX C BLOW-THROUGH ANALYSIS FOR CASE STUDY #2	88
APPENDIX D CHLORIDE CONCENTRATION AT TOP MAT OF REINFORCING STEEL WITH AN APPLIED SURFACE TREATMENT.....	99
APPENDIX E CHLORIDE CONCENTRATION AT BOTTOM MAT OF REINFORCING STEEL WITH AN APPLIED SURFACE TREATMENT.....	101
APPENDIX F CHLORIDE CONCENTRATION AT TOP MAT OF REINFORCING STEEL WITHOUT AN APPLIED SURFACE TREATMENT	103
APPENDIX G CHLORIDE CONCENTRATION AT BOTTOM MAT OF REINFORCING STEEL WITHOUT AN APPLIED SURFACE TREATMENT.....	105

LIST OF TABLES

Table 3-1: Monthly Temperature and Chloride Concentration Inputs for Chloride Concentration Analysis.....	18
Table 3-2: Concrete Exposure and Property Inputs for Chloride Concentration Analysis.....	20
Table 4-1: Questionnaire Survey Results	34
Table 4-2: Maximum Chloride Concentrations for a 2.0-in. OCD with a Surface Treatment	39
Table 4-3: Maximum Chloride Concentrations for a 2.5-in. OCD with a Surface Treatment	39
Table 4-4: Maximum Chloride Concentrations for a 3.0-in. OCD with a Surface Treatment	39
Table 4-5: Maximum Chloride Concentrations for a 2.0-in. OCD without a Surface Treatment.....	40
Table 4-6: Maximum Chloride Concentrations for a 2.5-in. OCD without a Surface Treatment.....	40
Table 4-7: Maximum Chloride Concentrations for a 3.0-in. OCD without a Surface Treatment.....	41
Table 4-8: Ranges of Parameters for Evaluation of Main Effects in Blow-through Analysis	43
Table 4-9: Ranges of Parameters for Evaluation of Interactions in Blow-through Analysis	47
Table 4-10: Parameter Combinations with Factor of Safety Less Than 3.0.....	50
Table 4-11: Blow-through Analysis Results for Various Scenarios for Case Study #1	54
Table 4-12: Blow-through Analysis Results for Various Scenarios for Case Study #2	57

LIST OF FIGURES

Figure 1-1: Schematic of hydrodemolition equipment.	2
Figure 1-2: Schematic of concrete removal below the top mat of reinforcing steel using hydrodemolition equipment.	3
Figure 3-1: Area of blow-through analysis between two longitudinal bars and two transverse bars in the bottom mat of reinforcing steel.	23
Figure 4-1: Simulated chloride concentrations at the top mat of reinforcement for a deck with a 2.0-in. OCD and a 3.375-in. removal depth with an applied surface treatment.	37
Figure 4-2: Simulated chloride concentrations at the bottom mat of reinforcement for a deck with a 2.0-in. OCD and a 3.375-in. removal depth with an applied surface treatment.	37
Figure 4-3: Simulated chloride concentrations at the top mat of reinforcement for a deck with a 2.0-in. OCD and a 3.375-in. removal depth without an applied surface treatment.	38
Figure 4-4: Simulated chloride concentrations at the bottom mat of reinforcement for a deck with a 2.0-in. OCD and a 3.375-in. removal depth without an applied surface treatment.	38
Figure 4-5: Main effect of transverse rebar spacing.	44
Figure 4-6: Main effect of concrete compressive strength.	44
Figure 4-7: Main effect of depth of removal below bottom of top reinforcing mat.	45
Figure 4-8: Main effect of orifice size.	45
Figure 4-9: Main effect of water pressure.	46
Figure 4-10: Main effect of jet angle.	46
Figure 4-11: Interaction between concrete compressive strength and transverse rebar spacing for water pressure of 10 ksi.	48
Figure 4-12: Interaction between concrete compressive strength and transverse rebar spacing for water pressure of 20 ksi.	49
Figure 4-13: Interaction between concrete compressive strength and transverse rebar spacing for water pressure of 30 ksi.	49
Figure 4-14: Interaction between concrete compressive strength and transverse rebar spacing for water pressure of 40 ksi.	50
Figure 4-15: Blow-through map for case study #1: (a) 0-350 ft, (b) 350-745 ft, (c) 745-1,075 ft, and (d) 1,075-1,425 ft.	52

Figure 4-16: Significant blow-through of the deck in case study #1.....	52
Figure 4-17: Significant efflorescence and cracking on the underside of the deck in case study #1.....	55
Figure 4-18: Blow-through map for case study #2: (a) 0-104.2 ft and (b) 104.2-208.5 ft.....	55
Figure 4-19: Insignificant blow-through of the deck in case study #2.	56
Figure 4-20: Insignificant efflorescence and cracking on the underside of the deck in case study #2.....	58

1 INTRODUCTION

1.1 Problem Statement

Chloride-induced corrosion of reinforcing steel is one of the leading causes of concrete bridge deck deterioration (Grace et al. 2004, Lees 1992, Mays 1992, Mindess et al. 2003, Suryavanshi et al. 1998, Zhang et al. 1998). Chloride ions, generally resulting from the application of deicing salts as part of winter bridge maintenance, can diffuse into the surface of a concrete bridge deck and interact with the embedded reinforcing steel. Steel reinforcement typically begins to corrode at a chloride concentration of 2.0 lb of chloride per cubic yard of concrete, forming expansive rust (Hema et al. 2004). As concrete is relatively weak in tension, the tensile forces exerted by the expansive rust cause the surrounding concrete to crack (Patnaik and Baah 2015). Eventually, such cracking can lead to delaminations and potholes on the bridge deck surface, which decrease the structural integrity, ride quality, and service life of the bridge deck (Patnaik and Baah 2015).

Repair of these distresses requires removal and replacement of the damaged concrete. One technique that is especially useful for partial-depth concrete removal is hydrodemolition (Hopwood et al. 2015, Momber 2005, Wenzlick 2002). This technique, which is becoming an increasingly common practice, involves removal of deteriorated concrete from the top surface of a concrete bridge deck using high-pressure water jets as illustrated in Figure 1-1 (Wenzlick 2002). Following removal of the old concrete, new concrete is placed to restore or increase, as needed, the original deck thickness and specified design strength (Wenzlick 2002). A surface

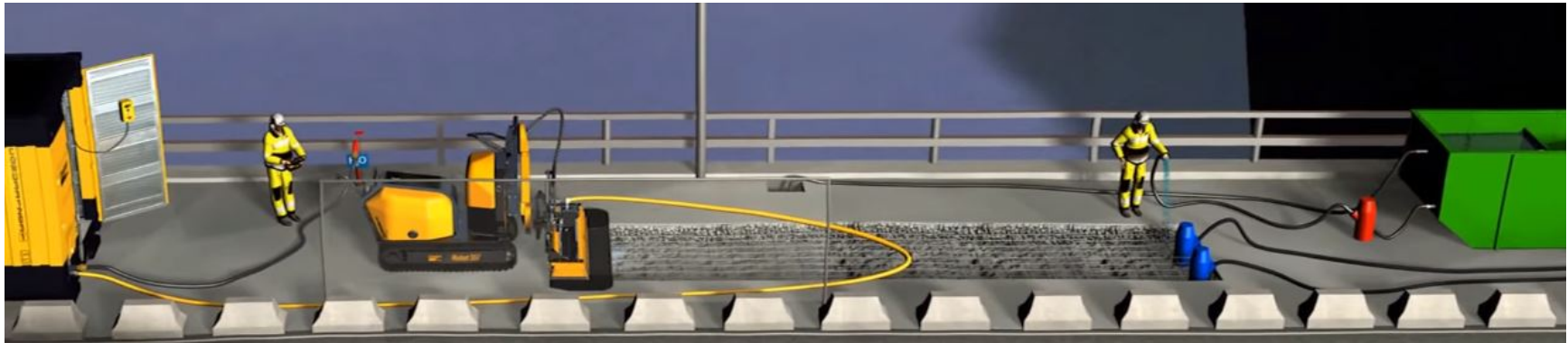


Figure 1-1: Schematic of hydrodemolition equipment.

treatment is commonly applied to the new deck surface to prevent future ingress of chloride ions and/or water (Birdsall et al. 2007, Hopwood et al. 2015, Swamy and Tanikawa 1993).

Unlike traditional concrete removal techniques such as milling, which is limited to depths shallower than the top mat of reinforcing steel (Guthrie et al. 2008), hydrodemolition can be used to remove concrete from around and even below the top mat of reinforcing steel as shown in Figure 1-2 (Wenzlick 2002). Thus, bridge decks that may no longer be suitable for repair using traditional concrete removal techniques, due to the development of critical chloride concentrations at depths deeper than the top mat of reinforcing steel, may still be good candidates for repair using hydrodemolition. In these cases, depending on the chloride concentrations at the time of hydrodemolition and the depth of concrete removal below the top mat of reinforcing steel, the service life of the deck may be significantly extended. Specifically, a sufficient quantity of chloride ions must be removed from the deck so that, after application of a

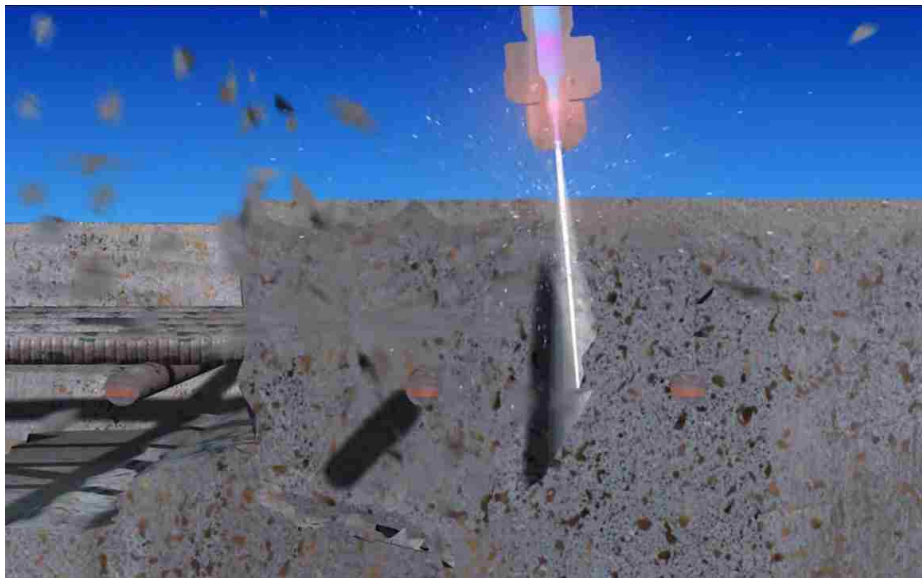


Figure 1-2: Schematic of concrete removal below the top mat of reinforcing steel using hydrodemolition equipment.

surface treatment preventing further chloride ingress, equilibration of the remaining chloride ions in the repaired deck does not result in a chloride concentration greater than or equal to 2.0 lb of chloride per cubic yard of concrete at the top or bottom mat of reinforcing steel. While the effects of treatment timing on deck service life have been analyzed for traditional repair techniques involving removal of concrete to depths shallower than the top mat of reinforcing steel (Guthrie et al. 2008), the effects of treatment timing on deck service life have not been analyzed for repair involving hydrodemolition of concrete to depths deeper than the top mat of reinforcing steel.

When hydrodemolition is used to remove concrete to depths deeper than the top mat of reinforcing steel, the high-pressure water jets can sometimes blow through the entire depth of a concrete bridge deck, which is a very undesirable outcome (Hopwood et al. 2015). Such “blow-throughs” result in several major problems. One is that falling concrete debris can cause personal injury to people and/or damage to property under the bridge. Another is that the holes in the deck are not only hazardous to construction workers but they prevent containment of the hydrodemolition water, which can be harmful to the environment if not properly treated prior to being released. Finally, the occurrence of blow-throughs can significantly increase the cost of bridge deck repair because of the requirement for additional formwork and concrete material. While blow-throughs have been observed to occur in deck sections characterized by extensive cracking and efflorescence, they can also occur without warning in a seemingly sound bridge deck. While some limited anecdotal information exists about potentially influential factors (ICRI 2014), structural analyses are needed to quantify the effects of water pressure, jet orifice size, angle of impact, reinforcement dimensions, and concrete compressive strength on the occurrence of blow-through during hydrodemolition.

1.2 Research Objectives and Scope

The objectives of this research were 1) to investigate the effects of hydrodemolition treatment timing on chloride concentration profiles in concrete bridge decks for depths of concrete removal below the top mat of reinforcing steel and 2) to investigate factors that influence the occurrence of blow-throughs in concrete bridge decks when hydrodemolition is used. The research results are intended to provide engineers with guidance about the latest timing of hydrodemolition that can maintain a chloride concentration level below 2.0 lb of chloride per cubic yard of concrete at the levels of both the top and bottom mats of reinforcing steel, as well as about conditions that may indicate a higher probability of blow-through during hydrodemolition. The scope of this research included a questionnaire survey of hydrodemolition companies to summarize common practices in the field, numerical modeling of chloride concentration to investigate hydrodemolition treatment timing on typical Utah bridge decks, and structural analysis to investigate factors that influence the occurrence of blow-throughs during hydrodemolition. In particular, the results of the questionnaire survey were used to identify appropriate inputs for the blow-through analysis.

1.3 Outline of Report

This report contains five chapters. This chapter defines the problem statement, introduces the research, and states the research objectives and scope. Chapter 2 provides background information obtained from a literature review about chloride-induced corrosion of reinforcing steel, removal of deteriorated concrete using hydrodemolition, and application of surface treatments to concrete bridge decks. Chapter 3 details the procedures for the questionnaire survey, chloride concentration analysis, and blow-through analysis, and Chapter 4 presents the

results of the survey and analyses. Chapter 5 provides a summary together with conclusions and recommendations resulting from this research.

2 BACKGROUND

2.1 Overview

Developed from a literature review performed for this research, the following sections discuss chloride-induced corrosion of reinforcing steel, removal of deteriorated concrete using hydrodemolition, and application of surface treatments to concrete bridge decks.

2.2 Chloride-Induced Corrosion of Reinforcing Steel

With time, the diffusion and accumulation of chloride ions in reinforced concrete causes a breakdown of the protective environment that concrete naturally provides for reinforcing steel. Typically, the threshold value at which chloride ions initiate corrosion of reinforcing steel is 2.0 lb of chloride per cubic yard of concrete (Hema et al. 2004). Diffusion occurs as chloride ions move in response to spatial differences in entropy (Mays 1992), traveling from areas of higher concentration to areas of lower concentration (Freeze and Cheery 1979). The chloride diffusion process in a bridge deck is initiated when salt solutions contact the concrete surface. In cold regions, such as Utah, chloride ions are introduced to the surface of bridge decks in the form of deicing salts. After dissolution in water, chloride ions can diffuse into the concrete matrix and disperse to areas of lower concentration over time (Arora et al. 1997). The depth of chloride penetration into concrete over a given time period is governed by the chloride diffusion coefficient and the chloride concentration gradient (Grace et al. 2004). The diffusion coefficient is a measure of the rate at which chloride ions can diffuse through the concrete over time, while

the concentration gradient shows how the ions are dispersed throughout the concrete matrix. Larger diffusion coefficients and higher concentration gradients allow the chloride ions to diffuse more rapidly through the concrete.

According to Fick's first law of diffusion, chloride ions will diffuse in the direction of decreasing chloride concentration (Poulsen and Mejlbro 2006). Therefore, chloride ions can diffuse in any direction, including upward and downward, depending on the chloride concentration gradient. Thus, when new chloride-free concrete is placed on top of an existing chloride-laden concrete bridge deck, for example, chloride ions present in the existing concrete will diffuse upwards through the new concrete and downwards through the existing concrete over time.

Especially in cold regions, winter road maintenance practices affect chloride concentrations at the surface of bridge decks through the application of deicing salts. With all other factors held constant, the surface chloride concentration for bridges that receive more deicing salt applications is higher than that of bridges that receive fewer deicing salt applications. Furthermore, precipitation leads to higher moisture contents within the concrete matrix, which causes higher diffusion coefficients and greater ionic conduction (Guthrie et al. 2006). However, lower temperatures reduce ionic mobility, which results in lower diffusion rates during periods of cold weather (Clark and Hawley 1966, Lewis 2001).

To a large degree, the water-cement ratio and degree of hydration of the concrete determine the properties of the concrete matrix. Specifically, diffusion is limited by the degree of saturation and continuity of the pore water within the concrete matrix (Survananshi et al. 1998). As the degree of saturation and continuity of the pore water increase, the rate of diffusion increases (Zhang et al. 1998). For a given concrete mixture, the external chloride loading and

cover thickness govern the time required for chloride ions to accumulate in critical concentrations near the reinforcing steel. Cover thicknesses for concrete bridge decks are typically in the range of 2.0 to 3.0 in. (relative to the transverse reinforcing steel) (Hema et al. 2004). In the top mat of reinforcement, the transverse steel is located above the longitudinal steel; in the bottom mat of reinforcement, the transverse steel is located below the longitudinal steel.

Diffusion of chloride ions through the concrete matrix can lead to corrosion of the embedded reinforcing steel, deterioration of the surrounding concrete, and failure of the structure if left untreated. Various treatments and rehabilitation methods may be employed to maintain the safety and serviceability of concrete bridge decks.

2.3 Removal of Deteriorated Concrete Using Hydrodemolition

Over time, chloride-induced corrosion necessitates rehabilitation of concrete bridge decks. The cost and extent of such work are dependent on the amount of deterioration that has occurred within the concrete. If the deterioration is limited to the concrete in the upper half of the deck, partial-depth repairs are appropriate. However, if the deterioration has extended into the lower half of the deck, full-depth repair is often necessary (Wenzlick 2002). Methods for removing deteriorated concrete from a bridge deck include jackhammering, milling, and hydrodemolition (Wenzlick 2002). While the first two methods generate harmful vibrations that can induce micro-cracking in the surrounding concrete and lead to further deterioration of the deck, hydrodemolition has proven to be less damaging to the existing concrete structure when used appropriately.

Hydrodemolition is the use of high-pressure water jets to remove deteriorated concrete from the surface of a structure (ICRI 2014). In the process of rehabilitating concrete bridge decks, new concrete is placed following hydrodemolition to restore or increase, as needed, the original deck thickness and specified design strength. Hydrodemolition is typically used for partial-depth repair rather than full-depth repair. The process involves use of fully-automated, high-pressure water jets with constant pressure, frequently exceeding 20,000 psi, to remove concrete from the top surface of the deck (Momber 2005). In some cases, concrete is removed to a predetermined depth, regardless of the degree of localized deterioration (Momber 2005). In other cases, a depth specification is not given, and the depth of concrete removal is governed mainly by the degree of deterioration (ICRI 2014); the high-pressure water jets are calibrated to remove low-strength and damaged concrete while leaving sound concrete in place on the concrete bridge deck (Wenzlick 2002). Therefore, in areas where concrete is in poor condition, concrete is removed to a greater depth. When the top mat of reinforcing steel is exposed, the hydrodemolition process also removes corrosion products, or rust, from the steel. One to four passes of the hydrodemolition jets are typically required to achieve the desired outcomes (Momber 2005).

Specific advantages and disadvantages apply to the use of hydrodemolition as part of the rehabilitation process for a concrete bridge deck. The main advantages of hydrodemolition include increased cost effectiveness, decreased time consumption, increased adhesion between the concrete substrate and new concrete, and decreased damage to the existing structure (Momber 2005, Wenzlick 2002). Removing deteriorated concrete from only the upper portion of the bridge deck decreases rehabilitation costs when compared to full-depth removal. Similarly, the high-pressure water jets can remove unsound concrete at a quicker rate than other methods,

such as jackhammering, which decreases the time necessary to complete rehabilitation (ICRI 2014, Wenzlick 2002). Adhesion between concrete layers increases as the greater exposed surface area of the substrate leads to improved mechanical interlock with the new concrete (Harries et al. 2013, ICRI 2014, Momber 2005); in particular, the increased pull-off strength of layers applied to hydrodemolished surfaces is a notable advantage of hydrodemolition compared to other concrete removal methods. Decreased damage to the existing structure is possible because the process does not generate harmful vibrations like jackhammering or milling (ICRI 2014, Wenzlick 2002).

The main disadvantages associated with hydrodemolition include environmental and safety concerns. Environmental concerns arise when even small quantities of the waste water, which has high levels of alkalinity and harmful solutes, bypass the collection system and enter the surrounding landscape (Momber 2005). The intensity of this problem is exacerbated when hydrodemolition is applied to bridges spanning water bodies or other environmentally sensitive areas. In these situations, extra care must be taken to also guard against blow-throughs, which can result from application of the high-pressure water jets to unsound concrete with extensive cracking, low-strength layers, or other defects (Hopwood 2015, ICRI 2014). Because of the possibility of waste water leakage and falling debris, blow-throughs pose both environmental and safety problems if special precautions are not taken (ICRI 2014). Specifically regarding safety, while people may be injured and/or property may be damaged by falling debris, the resulting holes in the bridge deck are also a significant hazard for construction personnel performing the rehabilitation work. Therefore, minimizing the occurrence of blow-throughs is critical.

2.4 Application of Surface Treatments to Concrete Bridge Decks

One method of effectively and economically disrupting the ingress of chloride ions and/or moisture is adding a surface treatment (Birdsall et al. 2007, Swamy and Tanikawa 1993). Following a rehabilitation method involving removal of deteriorated material and placement of new concrete, for example, a surface treatment can be applied to seal the rehabilitated concrete deck against further chloride ingress. In some cases, application of a surface treatment can be delayed after deck rehabilitation, but the maximum extension in service life of concrete bridge decks is obtained if surface treatments are placed before chloride concentrations have reached critical levels at the top mat of reinforcing steel (Birdsall et al. 2007, Guthrie et al. 2008, Zhang et al. 1998). To achieve the desired effect, appropriate materials, deck preparation techniques, and placement methods must be utilized (Basheer et al. 1998).

The materials generally used in surface treatments applied to concrete bridge decks include binders and aggregates. The binders are typically urethane, silicon-based, or epoxy products, which function both as adhesives and as sealants (Guthrie et al. 2005). In many instances, aggregates are mixed with or broadcast into the binders to provide skid resistance and protection of the binders from ultraviolet radiation (Guthrie et al. 2005).

Appropriate deck preparation is necessary to ensure adequate adhesion between the concrete substrate and the applied surface treatment (Pan et al. 2016). A concrete bridge deck surface should be cleaned and roughened, using shot blasting, for example, to facilitate increased bond strength between the concrete substrate and the surface treatment (Guthrie et al. 2005). Following this roughening process, all debris should be removed from the deck surface, and, depending on the moisture content of the concrete, the deck may also need to be dried (Guthrie et

al. 2005); the presence of moisture on the deck surface or in the substrate can significantly reduce the bond strength (Guthrie et al. 2005, Pan et al. 2016).

Proper placement methods should be practiced to ensure that the surface treatment performs according to its design. While the materials comprising the surface treatment may be adequate, improper construction can cause premature failure of the surface treatment (Pan et al. 2016). The age and water content of the concrete substrate, treatment application method, and amount of treatment material govern the effectiveness of the surface treatment (Pan et al. 2016). If the underlying concrete has been poorly constructed or mixed, the surface treatment will likely not perform properly (Pan et al. 2016). The surface treatment should be allowed adequate curing time and protection from traffic to prevent premature failure (Weyers et al. 1993).

2.5 Summary

Developed from a literature review performed for this research, this chapter discusses chloride-induced corrosion of reinforcing steel, removal of deteriorated concrete using hydrodemolition, and application of surface treatments to concrete bridge decks. With time, the diffusion and accumulation of chloride ions in reinforced concrete causes a breakdown of the protective environment that concrete naturally provides for reinforcing steel. Typically, the threshold value at which chloride ions initiate corrosion of reinforcing steel is 2.0 lb of chloride per cubic yard of concrete. The chloride diffusion process in a bridge deck is initiated when salt solutions contact the concrete surface. Diffusion of chloride ions through the concrete matrix can lead to corrosion of the embedded reinforcing steel, deterioration of the surrounding concrete, and failure of the structure if left untreated. Various treatments and rehabilitation methods may be employed to maintain the safety and serviceability of concrete bridge decks.

Methods for removing deteriorated concrete from a bridge deck include jackhammering, milling, and hydrodemolition. Hydrodemolition is the use of high-pressure water jets to remove deteriorated concrete from the surface of a structure. Specific advantages and disadvantages apply to the use of hydrodemolition as part of the rehabilitation process for a concrete bridge deck. The main advantages of hydrodemolition include increased cost effectiveness, decreased time consumption, increased adhesion between the substrate and new concrete, and decreased damage to the existing structure. The main disadvantages associated with hydrodemolition include environmental and safety concerns. Environmental concerns arise when even small quantities of the waste water, which has high levels of alkalinity and harmful solutes, bypass the collection system and enter the surrounding landscape. Extra care must be taken to also guard against blow-throughs, which can result from application of the high-pressure water jets to unsound concrete with extensive cracking, low-strength layers, or other defects.

One method of effectively and economically disrupting the ingress of chloride ions and/or moisture is adding a surface treatment. Following a rehabilitation method involving removal of deteriorated material and placement of new concrete, for example, a surface treatment can be applied to seal the rehabilitated concrete deck against further chloride ingress. To achieve the desired effect, appropriate materials, deck preparation techniques, and placement methods must be utilized.

3 EXPERIMENTAL METHODOLOGY

3.1 Overview

The objectives of this research were met by conducting a questionnaire survey of hydrodemolition companies, performing numerical modeling of chloride concentration to investigate hydrodemolition treatment timing on typical Utah bridge decks, and using structural analysis to investigate factors that influence the occurrence of blow-throughs during hydrodemolition. This chapter describes the methodology utilized in the survey, explains the procedures utilized for numerical modeling of chloride concentration, and details the blow-through analyses.

3.2 Questionnaire Survey

A questionnaire survey was conducted by telephone and email to assess current practices of selected hydrodemolition companies that rehabilitate concrete bridge decks throughout the country. The survey findings were used to design the numerical experiments performed to investigate factors that influence the occurrence of blow-throughs in concrete bridge decks when hydrodemolition is used. Various hydrodemolition companies were selected based on their experience with hydrodemolition of bridge decks in climates and conditions similar to those in Utah, where deicing salts are routinely applied to bridges as part of winter maintenance.

A total of five persons, who were typically the managers of the hydrodemolition companies, participated in the survey. Each survey respondent was asked the following questions regarding hydrodemolition procedures for concrete bridge deck rehabilitation:

- Which states are serviced by the hydrodemolition company?
- What nozzle type is used for hydrodemolition of concrete bridge decks?
- What nozzle (orifice) size is typically used for hydrodemolition of concrete bridge decks?
- What water pressure is typically used for hydrodemolition of concrete bridge decks?
- What is the flow rate of the water through the nozzle jet?
- What is the standoff distance, or height that the hydrodemolition nozzle operates above the bridge deck?
- At what angle relative to the bridge deck surface does the hydrodemolition jet typically operate?
- What is the typical transverse speed of hydrodemolition jets on concrete bridge decks?
- How often do blow-throughs of the concrete bridge deck occur during hydrodemolition?

The answers to these questions were compiled to assess the current bridge deck rehabilitation practices of these hydrodemolition companies.

3.3 Chloride Concentration Analysis

Numerical modeling was performed to investigate the effects of hydrodemolition treatment timing on chloride concentration profiles in concrete bridge decks for depths of concrete removal below the top mat of reinforcing steel. Based on communications with UDOT engineers to determine current practice, appropriate ranges of removal and overlay depths were

selected for use in the modeling process. In addition, typical ranges in bridge deck thickness, original cover depth (OCD), and depth and size of steel reinforcement were selected.

Numerical modeling of chloride concentration was performed using a software program developed by the National Institute of Standards and Technology (NIST) (Bentz 2016). The program uses the one-dimensional approximation for diffusion based on Fick's second law, shown as Equation 3-1, to simulate the diffusion of chlorides through concrete (Poulsen and Mejlbro 2006):

$$\frac{\partial C}{\partial t} = D \frac{\partial^2 C}{\partial x^2} \quad (3-1)$$

where:

C = chloride concentration, mol/m³

t = time, s

D = diffusion coefficient, m²/s

x = position, m

The program considers several user-specified internal and external variables that affect chloride diffusion through concrete. Among the internal variables are concrete properties such as water-cement ratio, degree of hydration, volume fraction of aggregate, air content, diffusion coefficients, and initial chloride concentration. The values of these parameters were specified in this research to be the same for both the original concrete in the bridge deck and the concrete placed to restore the deck following hydrodemolition. The external variables include average monthly temperature, surface chloride concentration, and unexposed boundary condition.

Average monthly temperatures used in the numerical modeling program are shown in Table 3-1.

Table 3-1: Monthly Temperature and Chloride Concentration Inputs for Chloride Concentration Analysis

Month	Temperature (°C)	Chloride, C_s (mol/liter)
January	-2.3	4.273
February	1.2	3.865
March	5.4	3.326
April	9.8	2.800
May	14.9	2.429
June	20.6	2.311
July	25.5	2.479
August	24.2	2.887
September	18.4	3.427
October	11.8	3.952
November	4.9	4.324
December	-1.3	4.441

The initial chloride concentration of the new concrete was assumed to be 0.0 g chloride/g cement, and the chloride concentration at the unexposed boundary condition was specified as “constant at zero” to reflect the absence of stay-in-place metal forms, which are no longer commonly used in Utah, on the bottom of the bridge deck (Guthrie et al. 2006). At the exposed boundary condition, a cyclic loading of chlorides on the top surface of the bridge deck was specified to simulate the seasonal exposure of bridges in Utah to deicing salt in the absence of a surface treatment; after a simulated surface treatment application, the chloride concentration at the top surface of the bridge deck was specified to be zero, as the treatment, if maintained over time, should prevent future ingress of chloride ions and/or water. The function used to approximate the surface chloride concentration through a typical year is given in Equation 3-2:

$$C = 3.38 + 1.07 \cdot \cos\left(\frac{\pi \cdot t}{6}\right) \quad (3-2)$$

where:

C = chloride concentration of pore water for month t , mol/L

t = month of year from 1 to 12 to represent January to December, respectively.

This function was developed by previous researchers at Brigham Young University (BYU) (Birdsall et al. 2007). The development process involved measurement of average chloride concentration profiles for several concrete bridge decks in Utah and use of numerical modeling to iteratively determine a single chloride surface concentration model that provided the best possible matches between simulated and measured chloride data (Birdsall et al. 2007).

As shown in Table 3-2, specific inputs for the numerical modeling program were determined from local climatic conditions and with assistance from personnel at NIST. The beginning month of exposure shown in Table 3-2 refers to the first month of the winter season when snow and icy conditions generally necessitate application of deicing salts to roads and bridges to increase driver safety. The member thickness is the deck thickness, and the water-cementitious material ratio, volume fraction of aggregate, air content, and diffusion coefficient are specified to match typical concrete mixture designs used for bridge deck construction in Utah (Birdsall et al. 2007). (To achieve a constant diffusion coefficient with time in the simulations, the constant diffusion coefficient was set to the desired value, and the initial diffusion coefficient was set to 0, as required in the numerical modeling program.) The time before exposure begins is set to reflect the expectation that a deck would not be exposed to deicing salts until at least 28 days following construction. The degree of hydration, empirical coefficient, activation energy, Langmuir isotherm constants, rate constants for binding, and cement compound contents are specified according to recommendations from NIST personnel. The external chloride concentration values are computed from Equation 3-2, which generates higher chloride

Table 3-2: Concrete Exposure and Property Inputs for Chloride Concentration Analysis

Property	Value
Beginning Month of Exposure	October
Member Thickness (m)	0.203, 0.229, or 0.254
Water-Cementitious Material Ratio, w/cm	0.44
Degree of Hydration	0.8
Volume Fraction of Aggregate (%)	65
Air Content (%)	6
Initial Chloride Concentration of Concrete (g Chloride/ g Cement)	0
Initial Diffusion Coefficient, D_i (m^2/s)	0
Constant Diffusion Coefficient, D_{inf} (m^2/s)	1.30E-11
Empirical Coefficient, m	0.6
Time before Exposure Begins (days)	28
Ratio of Surface-to-Bulk Diffusion Coefficients	1
Thickness of Surface Layer (mm)	0
Activation Energy for Diffusion (kJ/mol)	40
Langmuir Isotherm Alpha Constant	1.67
Langmuir Isotherm Beta Constant	4.08
Rate Constant of Binding (s^{-1})	1.00E-07
C ₃ A Content of Cement (%)	5
C ₄ AF Content of Cement (%)	5
Rate Constant for Aluminate Reactions with Chloride (s^{-1})	1.00E-08

concentrations for the months of October through February because these are the months that typically require deicing salt applications. Selection of the indicated values ensured as much consistency as possible with previous research performed at BYU (Birdsall et al. 2007, Guthrie et al. 2008).

For the specified bridge deck thicknesses of 8.0, 9.0, and 10.0 in., corresponding OCDs of 2.0, 2.5, and 3.0 in. (relative to the transverse reinforcing steel) were used in the simulations. Specific removal depths chosen for numerical modeling were computed as the sum of a given OCD, the diameter of a No. 5 reinforcing bar (0.625 in.) typically comprising the top mat, and an

additional depth of 0.75 in. below the top mat that is expected to occur as hydrodemolition contractors meet the required removal depth of 0.50 in. specified by UDOT. Therefore, the total removal depths, which were 3.375, 3.875, and 4.375 in., effectively represent the “worst-case” scenario for the numerical modeling; with the transverse bar being used as the datum in the top mat of reinforcing steel, the removal depths are shallower than if the longitudinal bar had been used, and the reduced removal depth corresponds to a greater amount of chloride-contaminated concrete being left in the bridge deck.

Besides removing potentially chloride-contaminated concrete from immediately around the reinforcing steel, extending the depth of concrete removal below the top mat of reinforcing steel also allows mechanical interlock with the new concrete placed after hydrodemolition. The concrete, which usually has a nominal maximum aggregate size of 0.75 in., can flow under the reinforcing steel and thereby largely eliminate the possibility of debonding from the surface of the original concrete.

Using these parameters, each simulation differed based on total duration of chloride exposure, time at which hydrodemolition is performed, OCD, depth of removal by the high-pressure water jets, and application of a surface treatment on the rehabilitated concrete deck. With these variables accounted for, extensive numerical modeling of chloride concentration profiles was performed. Specifically, crossing the various levels of the experimental factors in a full-factorial structure generated a total of 36 unique combinations, or scenarios. Specifically, the experimentation included OCDs of 2.0, 2.5, and 3.0 in. (with corresponding removal depths of 3.375, 3.875, and 4.375 in.), treatment times of 25, 30, 35, 40, 45, and 50 years following deck construction; and the presence or absence of an applied surface treatment. In the modeling, all aspects of rehabilitation, including hydrodemolition, placement of new concrete, and application

of a surface treatment, as applicable, were assumed to occur at the same time. The numerical modeling for each scenario was performed for a simulated 75-year service life as recommended by the Federal Highway Administration (FHWA 2011).

Modeling of the decks without treatment was performed first to develop a baseline chloride concentration profile to which the chloride concentration profiles for various treatment times were compared. To develop the baseline profile, treatment timing was set at 1,000,000 days to ensure that the treatment would not affect the numerical modeling results during the simulation period. Modeling was then performed for each unique combination of OCD, treatment time, and surface treatment application to produce chloride concentration profiles that would be expected after rehabilitation was performed. The latest timing of rehabilitation that maintained a chloride concentration level below 2.0 lb of chloride per cubic yard of concrete at the levels of both the top and bottom mats of reinforcing steel was identified for each unique combination of OCD and surface treatment application. Appendix A includes images of the numerical modeling program with sample inputs for rehabilitation with a surface treatment application performed at a bridge deck age of 25 years.

3.4 Blow-through Analysis

For this research, a spreadsheet was developed to investigate six modes of failure, or blow-through, that can potentially be experienced by a concrete bridge deck during hydrodemolition. These modes of failure include bending, one-way shear, and two-way shear, each of which is analyzed in both the orientation where the length is greater than the width and in the orientation where the length is smaller than the width. For any of these failure modes, if the capacity of the concrete deck section is less than the forces applied by the high-pressure water jets, blow-through can be expected. The factor of safety against blow-through is calculated as the

shear or moment capacity of the simulated concrete deck section divided by the shear force or moment imparted by the high-pressure water jets.

In the spreadsheet, the concrete between two longitudinal bars and two transverse bars within the bottom mat of reinforcing steel was analyzed using the Euler-Bernoulli simplified beam theory (Gere and Goodno 2013). Figure 3-1 shows the area of analysis in the plane of the bottom mat of reinforcing steel, with the length of the beam being equal to the spacing between longitudinal reinforcing bars and the width of the beam being equal to the spacing between transverse reinforcing bars. The height of the beam was defined as the vertical distance from the middle of the longitudinal bar in the bottom mat of reinforcing steel to the scarified concrete surface between the top and bottom mats of reinforcing steel; any concrete below the bottom mat of reinforcing steel was disregarded in the analysis. Defining the beam height with reference to the longitudinal bar instead of the transverse bar in the bottom mat effectively represents the “worst-case” scenario for the analysis; because the longitudinal bar is positioned just above the transverse bar within the bottom mat of reinforcing steel, the beam height is lower for a given removal depth than if the transverse bar had been used, and the lower beam height corresponds

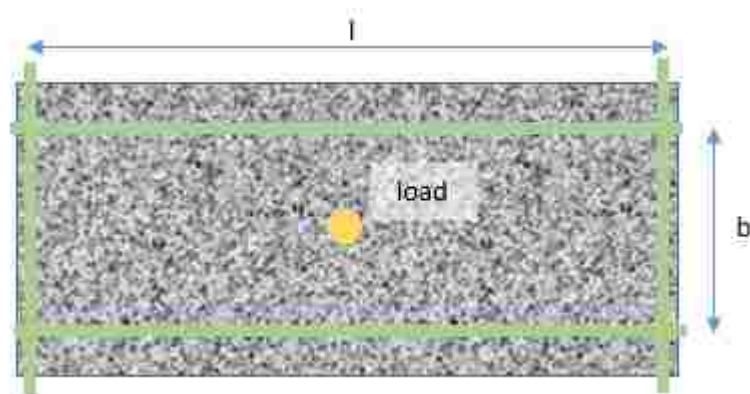


Figure 3-1: Area of blow-through analysis between two longitudinal bars and two transverse bars in the bottom mat of reinforcing steel.

to a higher probability of blow-through during hydrodemolition. (Because the top mat of reinforcing steel is above the top of the scarified concrete, it was not included in the analysis; although the physical presence of the top mat of reinforcing steel may prevent point loading of the beam in certain locations, it is not otherwise expected to affect the occurrence of blow-throughs.) As a simplification in this research, the concrete within the beam was assumed to be intact, without cracking or other distresses, and was also assumed to have homogenous mechanical properties, such as compressive strength. However, the perimeter of the beam was assumed to be cracked on all four sides and was assumed to be simply supported along two parallel sides coinciding with the two longitudinal bars or the two transverse bars, depending on the analysis; because this “worst-case” approach disregards the structural benefits of possible concrete continuity across the reinforcing steel, the analysis yields deliberately conservative results in this respect.

Several calculations were required in the analysis of the simulated concrete beam, including those for modulus of rupture, moment of inertia, maximum moment, cracking moment, maximum shear force, one-way shear strength, and two-way shear strength. The modulus of rupture was calculated using Equation 3-3 (McCormac and Brown 2015):

$$f_r = 7.5\lambda\sqrt{f'_c} \quad (3-3)$$

where:

f_r = modulus of rupture of the concrete beam, psi

λ = correction for unit weight of the concrete based on the type of concrete ($\lambda = 1$ for normal concrete, $\lambda = 0.85$ for sand-lightweight concrete, and $\lambda = 0.75$ for all-lightweight concrete)

f_c = compressive strength of the concrete, psi

The moment of inertia for analysis in the cases where the length was greater than the width and where the length was smaller than the width was computed using Equation 3-4 (McCormac and Brown 2015):

$$I = \frac{bh^3}{12} \quad (3-4)$$

where:

I = moment of inertia of the concrete beam, in.⁴

b = horizontal width of the concrete beam, in.

h = vertical distance from the middle of the longitudinal bar in the bottom mat of reinforcing steel to the top of the scarified surface, in.

The maximum moment experienced by the beam was calculated using Equation 3-5 (McCormac and Brown 2015):

$$M_{max} = \frac{P \sin \theta L}{4} \quad (3-5)$$

where:

M_{max} = maximum moment experienced by the concrete beam, ft-lb

P = point load exerted on the deck from the high-pressure water jet, lb

θ = angle between the jet and the deck surface with respect to vertical (i.e. 0 degrees is perpendicular to the horizontal plane of the deck surface),

degrees

L = horizontal length of the concrete beam, in.

The cracking moment of the concrete beam was calculated using Equation 3-6 (McCormac and Brown 2015):

$$M_{cr} = \frac{f_r I}{y} \quad (3-6)$$

where:

M_{cr} = cracking moment of the concrete beam, ft-lb

f_r = modulus of rupture of the concrete beam, psi

I = moment of inertia, in.⁴

y = vertical distance to the neutral axis of the beam from the middle of the longitudinal bar on the bottom mat of reinforcing steel, in.

The maximum shear force experienced by the beam was calculated using Equation 3-7 (McCormac and Brown 2015):

$$V_{max} = \frac{P \sin \theta}{2} \quad (3-7)$$

where:

V_{max} = maximum shear force experienced by the concrete beam, lb

P = point load exerted on the deck surface from the high-pressure water jet, lb

θ = angle between the jet and the deck surface with respect to vertical (i.e. 0 degrees is perpendicular to the horizontal plane of the deck surface), degrees

The one-way shear strength of the beam was computed using Equation 3-8 (McCormac and Brown 2015):

$$V_{c1} = 2\lambda\sqrt{f'_c}bh \quad (3-8)$$

where:

V_{c1} = one-way shear strength of the concrete beam, lb

λ = correction for unit weight of the concrete based on the type of concrete ($\lambda = 1$ for normal concrete, $\lambda = 0.85$ for sand-lightweight concrete, and $\lambda = 0.75$ for all-lightweight concrete)

f'_c = compressive strength of the concrete, psi

b = horizontal width of the concrete beam, in.

h = vertical distance from the middle of the longitudinal bar in the bottom mat of reinforcing steel to the top of the scarified surface, in.

The two-way shear strength, or punching shear strength, of the concrete beam was calculated using Equation 3-9 (McCormac and Brown 2015):

$$V_{c2} = 4\lambda\sqrt{f'_c}bh \quad (3-9)$$

where:

V_{c2} = two-way shear strength, or punching shear, of the concrete beam, lb

λ = correction for unit weight of the concrete based on the type of concrete ($\lambda = 1$ for normal concrete, $\lambda = 0.85$ for sand-lightweight concrete, and $\lambda = 0.75$ for all-lightweight concrete)

f_c = compressive strength of the concrete, psi

b = horizontal width of the concrete beam, in.

h = vertical distance from the middle of the longitudinal bar in the bottom mat of reinforcing steel to the top of the scarified surface, in.

The bridge deck parameters that were used as inputs in the blow-through analysis are bridge deck thickness, OCD, reinforcing bar size, longitudinal rebar spacing, transverse rebar spacing, type of concrete, concrete compressive strength, and removal depth. The bridge deck thickness typically varies from 7.0 to 10.0 in., with OCD values ranging from 2.0 to 3.0 in. The reinforcing bar size for bridge decks usually ranges from No. 4 to No. 10, and the transverse and longitudinal bars are assumed to be the same size in the analysis. Typically, the longitudinal bar spacing is 12 in., while the transverse bar spacing ranges from 6 to 12 in. The types of concrete that can be evaluated in the analysis include normal-weight, sand-lightweight, and all-lightweight concrete. The concrete compressive strength should be in the range of 1,000 to 9,000 psi, and it should be measured prior to hydrodemolition; if cores cannot be tested, estimates of the compressive strength may be obtained using a nondestructive device such as the Schmidt rebound hammer, for example. The removal depth ranges from 0.25 to 1.50 in. below the bottom of the transverse bar in the top mat of reinforcing steel.

The hydrodemolition equipment parameters that were used as inputs in the blow-through analysis are orifice size, water pressure, and angle of jet with respect to vertical. The ranges of these parameters were selected using the results of the questionnaire survey. The orifice diameter typically ranges from 0.10 to 0.25 in.; while smaller diameters can be used, diameters larger than 0.25 in. are not recommended for hydrodemolition of concrete bridge decks. Water pressure

varies from 10,000 to 40,000 psi. The angle of the jet ranges from 0 to 90 degrees, with the jet angle being set at 0 degrees if the jet is completely perpendicular to the bridge deck. In the blow-through analysis, the high-pressure water jet is assumed to have a cross-sectional diameter equal to the orifice diameter as it contacts the deck surface, and the force of the jet on the deck surface is therefore calculated as the product of the orifice area and the water pressure.

Following development of the spreadsheet, numerical experiments were performed to investigate factors that influence the occurrence of blow-throughs in concrete bridge decks when hydrodemolition is used. In one experiment, the main effect of each input variable on the occurrence of blow-throughs was evaluated by sequentially changing the value of the given variable across a typical range while holding the values of all other variables constant. In another experiment, the interactions among selected input variables were evaluated through a full-factorial experimental design set up to specifically simulate conditions representative of current UDOT practice. For the full-factorial experiment, the remaining concrete thickness above the bottom mat of reinforcing steel was held constant at 2.0 in., representing a removal depth of 0.75 in. below the bottom of the top mat of reinforcing steel; this is the removal depth that will likely result from the 0.50-in. removal depth typically specified by UDOT for hydrodemolition of concrete bridge decks.

Finally, the blow-through analysis was applied to two case studies on bridge decks in northern Utah that were rehabilitated using hydrodemolition. One bridge deck, which was constructed in 1972 and rehabilitated in 2015 at an age of 43 years, experienced significant blow-throughs; the other bridge deck, which was constructed in 1988 and rehabilitated in 2016 at an age of 28 years, experienced insignificant blow-throughs. In each case study, possible values of input variables were selected from bridge plans provided by UDOT, photographs and

measurements taken during and after hydrodemolition, and information obtained from the hydrodemolition contractors. Specifically, supporting information from the bridge plans is given in Appendices B and C for case studies #1 and #2, respectively. Compilation of this information allowed development of expected “worst-case” scenarios that were then investigated for each deck using the blow-through analysis.

3.5 Summary

The objectives of this research were met by conducting a questionnaire survey of hydrodemolition companies, performing numerical modeling of chloride concentration to investigate hydrodemolition treatment timing on typical Utah bridge decks, and using structural analysis to investigate factors that influence the occurrence of blow-throughs during hydrodemolition. This chapter describes the methodology utilized in the survey, explains the procedures utilized for numerical modeling of chloride concentration, and details the blow-through analyses.

A questionnaire survey was conducted by telephone and email to assess current practices of selected hydrodemolition companies that rehabilitate concrete bridge decks throughout the country. The survey findings were used to design the numerical experiments performed to investigate factors that influence the occurrence of blow-throughs in concrete bridge decks when hydrodemolition is used. A total of five survey participants, who were typically the managers of the hydrodemolition companies, responded to the survey, and their answers were compiled to assess the current bridge deck rehabilitation practices of these hydrodemolition companies.

Numerical modeling was performed to investigate the effects of hydrodemolition treatment timing on chloride concentration profiles in concrete bridge decks for depths of concrete removal below the top mat of reinforcing steel. Based on communications with UDOT

engineers to determine current practice, appropriate ranges of removal and overlay depths were selected for use in the modeling process. Crossing the various levels of the experimental factors in a full-factorial structure generated a total of 36 unique combinations, or scenarios. Modeling of the decks without treatment was performed first to develop a baseline chloride concentration profile to which the chloride concentration profiles for various treatment times were compared. Modeling was then performed for each unique combination of OCD, treatment time, and surface treatment application to produce chloride concentration profiles that would be expected after rehabilitation was performed. The latest timing of rehabilitation that maintained a chloride concentration level below 2.0 lb of chloride per cubic yard of concrete at the levels of both the top and bottom mats of reinforcing steel was identified for each unique combination of OCD and surface treatment application.

For this research, a spreadsheet was developed to investigate six modes of failure, or blow-through, that can potentially be experienced by a concrete bridge deck during hydrodemolition. These modes of failure include bending, one-way shear, and two-way shear, each of which is analyzed in both the orientation where the length is greater than the width and in the orientation where the length is smaller than the width. For any of these failure modes, if the capacity of the concrete deck section is less than the forces applied by the high-pressure water jets, blow-through can be expected. The factor of safety against blow-through is calculated as the shear or moment capacity of the concrete section divided by the shear force or moment imparted by the high-pressure water jets. Several calculations were required in the analysis of the simulated concrete beam, including those for modulus of rupture, moment of inertia, maximum moment, cracking moment, maximum shear force, one-way shear strength, and two-way shear strength. The bridge deck parameters that were used as inputs in the blow-through analysis are

bridge deck thickness, OCD, reinforcing bar size, longitudinal rebar spacing, transverse rebar spacing, type of concrete, concrete compressive strength, and removal depth. The hydrodemolition equipment parameters that were used as inputs in the blow-through analysis are orifice size, water pressure, and angle of jet. Following development of the spreadsheet, numerical experiments were performed to investigate factors that influence the occurrence of blow-throughs in concrete bridge decks when hydrodemolition is used. Finally, the blow-through analysis was applied to two case studies on bridge decks in northern Utah that were rehabilitated using hydrodemolition.

4 RESULTS AND ANALYSIS

4.1 Overview

This chapter presents the results of the questionnaire survey, chloride concentration analysis, and blow-through analysis performed in this research.

4.2 Questionnaire Survey

The responses received in the questionnaire survey conducted to assess current practices of selected hydrodemolition companies are shown in Table 4-1. While some respondents indicated that certain parameters vary, depending on the project, the information in Table 4-1 is valuable for understanding typical practices and was used to design the numerical experiments performed to investigate factors that influence the occurrence of blow-throughs in concrete bridge decks when hydrodemolition is used.

The survey responses indicate that both oscillating and rotating nozzle types are used in hydrodemolition of concrete bridge decks. An oscillating nozzle oscillates in the longitudinal direction as it moves transversely across the deck along a track while inclined at a fixed angle that sprays the water jet in the direction of transverse movement (ICRI 2014). A rotating nozzle rotates about its center while maintaining a slight fixed angle with respect to its vertical axis as it moves transversely across the deck along a track. In the past, hydrodemolition projects involving concrete bridge decks typically used an oscillating nozzle; however, current practice is moving

Table 4-1: Questionnaire Survey Results

Company	States Serviced	Nozzle Type	Orifice Size (in.)	Water Pressure (ksi)	Flow Rate (gpm)	Standoff Distance (in.)	Jet Angle (degrees)	Transverse Speed (fps)	Blow-through
A	HI, MA, NJ, UT	Oscillating	Varies	10-40	Unknown	Varies	Unknown	Varies	Occurs Regularly
B	Midwest, TX	Oscillating	0.25	12-20	50-70	2.0	20	Varies	Occurs Regularly
C	Midwest, AK, CA, WA	Rotating	0.10	15-30	40	< 1.0	Unknown	Varies	Occurs Regularly
D	GA, LA, MI, NY, OH, UT	Rotating	0.10	34	48	0.5	Unknown	0.5	Occurs Regularly
E	FL, NV, UT	Oscillating	0.10	20	43	1.0	0-15	Varies	Occurs Regularly

towards use of the more efficient rotating nozzle. A typical orifice size is either 0.10 in. or 0.25 in, with most of the respondents using 0.10 in. Some respondents indicated that an orifice size of 0.25 in. is inappropriate for hydrodemolition of concrete bridge decks because the greater force exerted by the high-pressure water jets with a larger orifice size increases the likelihood of blow-throughs. The water pressure ranges from 10 to 40 ksi, and flow rates generally range from 40 to 70 gallon per minute. The standoff distance, or the height that the hydrodemolition nozzle operates above the bridge deck, varies between 0.5 and 2.0 in., and the maximum jet angle relative to vertical is reported to be 15 or 20 degrees. While one respondent indicated that the transverse speed of the water jet is about 0.5 fps, all other respondents indicated that it varies by project.

All survey participants reported that blow-throughs are a common occurrence when using hydrodemolition on concrete bridge decks. A few mentioned that blow-throughs are most common on bridge decks with efflorescence on the underside of the deck, which is usually an indication that the deck has experienced extensive cracking and may have high chloride concentrations. All of the survey participants provide hydrodemolition services in states with harsh winter climates, similar to Utah, which necessitates the use of deicing salts on bridge decks and other roadways to ensure a higher level of driver safety when temperatures are below freezing. As previously discussed in Chapters 1 and 2, chloride ions from the deicing salts corrode the reinforcing steel and deteriorate the surrounding concrete. Blow-throughs can then occur as the high-pressure water jets break through the unsound concrete and corroded reinforcing steel.

4.3 Chloride Concentration Analysis

The numerical modeling performed to investigate the effects of hydrodemolition treatment timing on chloride concentration profiles in concrete bridge decks for depths of concrete removal below the top mat of reinforcing steel generated chloride concentration profiles through a 75-year service life given a specific OCD, treatment time, and surface treatment usage. From these profiles, graphs of chloride concentration through time at the levels of both the top and bottom mats of reinforcing steel were prepared for each OCD value and surface treatment usage included in the modeling. Examples of graphs prepared for the top and bottom mats of reinforcing steel are given in Figures 4-1 and 4-2, respectively, for a bridge deck with a 2.0-in. OCD, a 3.375-in. removal depth, and an applied surface treatment, while similar graphs for the same conditions but without an applied surface treatment are given in Figures 4-3 and 4-4. Simulated treatment times are shown at 5-year intervals from 25 to 50 years of deck age, which is typical of current practice in the state of Utah.

The full sets of figures are provided in Appendices D through G. For each treatment year, these figures were used to determine the maximum chloride concentration that would occur at both mats of reinforcing steel after hydrodemolition and the deck age at which these maximum values occurred. In addition, when the maximum chloride concentration was greater than the threshold of 2.0 lb of chloride per cubic yard of concrete, the deck age at which the threshold was reached was also determined.

Tables 4-2 to 4-7 summarize the results obtained for the 36 unique scenarios that were produced from crossing the various levels of the experimental factors. Consistent with the numerical modeling, the treatment years and deck ages shown in the tables are rounded to the

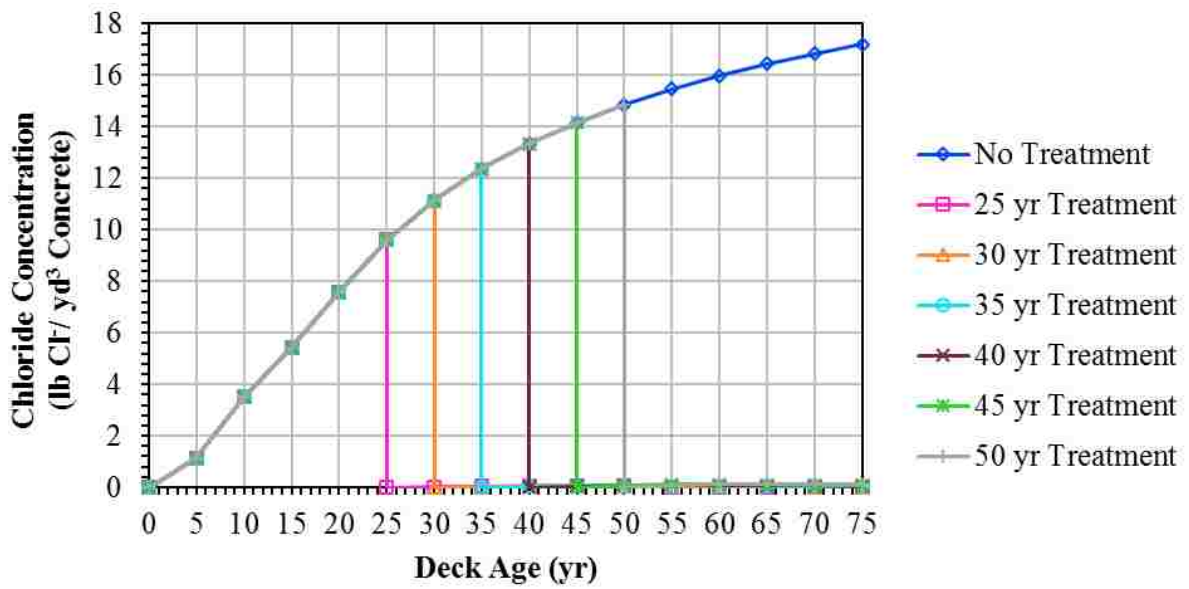


Figure 4-1: Simulated chloride concentrations at the top mat of reinforcement for a deck with a 2.0-in. OCD and a 3.375-in. removal depth with an applied surface treatment.

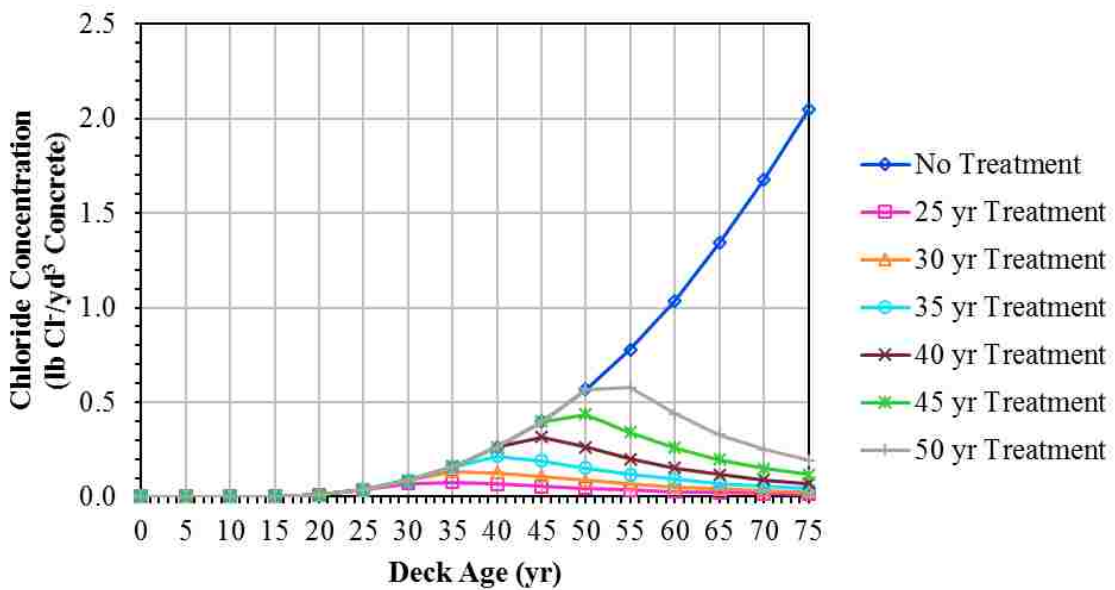


Figure 4-2: Simulated chloride concentrations at the bottom mat of reinforcement for a deck with a 2.0-in. OCD and a 3.375-in. removal depth with an applied surface treatment.

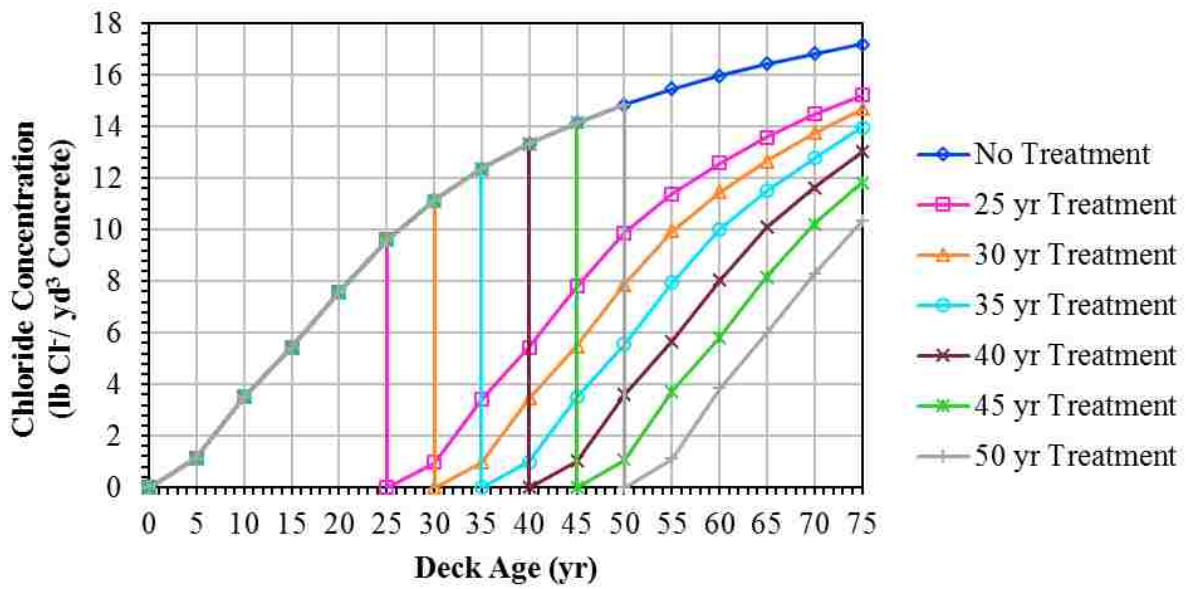


Figure 4-3: Simulated chloride concentrations at the top mat of reinforcement for a deck with a 2.0-in. OCD and a 3.375-in. removal depth without an applied surface treatment.

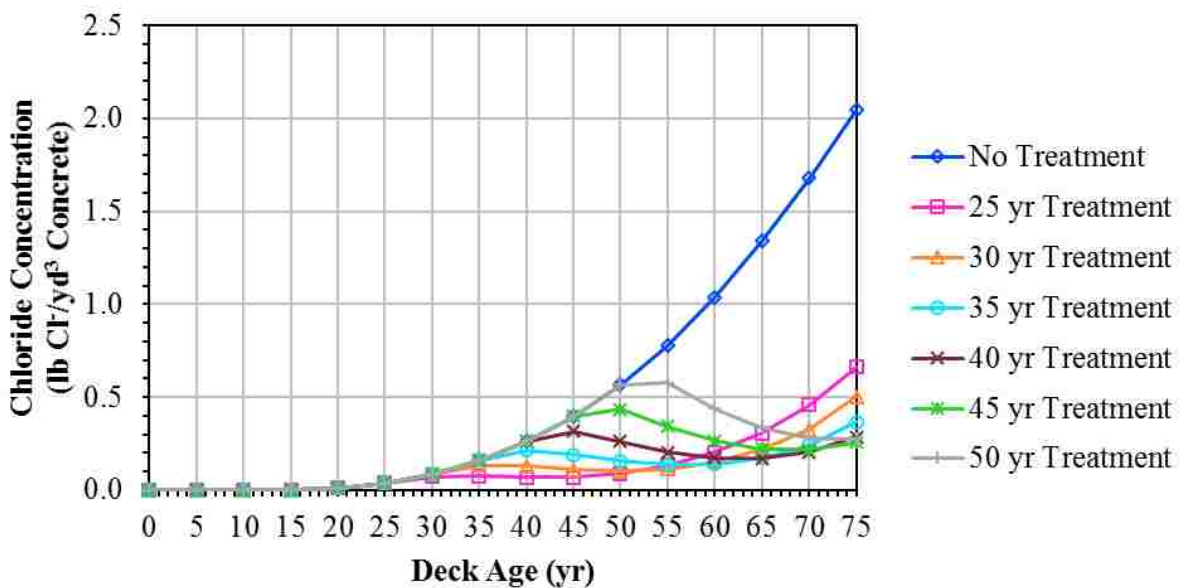


Figure 4-4: Simulated chloride concentrations at the bottom mat of reinforcement for a deck with a 2.0-in. OCD and a 3.375-in. removal depth without an applied surface treatment.

Table 4-2: Maximum Chloride Concentrations for a 2.0-in. OCD with a Surface Treatment

Treatment Year	Maximum Chloride Concentration after Treatment at Top Mat (lb Cl ⁻ /yd ³ Concrete)	Year of Maximum Value at Top Mat	Maximum Chloride Concentration after Treatment at Bottom Mat (lb Cl ⁻ /yd ³ Concrete)	Year of Maximum Value at Bottom Mat
25	0.04	40	0.08	35
30	0.06	45	0.13	35
35	0.07	50	0.21	40
40	0.09	55	0.32	45
45	0.12	60	0.44	50
50	0.15	65	0.58	55

Table 4-3: Maximum Chloride Concentrations for a 2.5-in. OCD with a Surface Treatment

Treatment Year	Maximum Chloride Concentration after Treatment at Top Mat (lb Cl ⁻ /yd ³ Concrete)	Year of Maximum Value at Top Mat	Maximum Chloride Concentration after Treatment at Bottom Mat (lb Cl ⁻ /yd ³ Concrete)	Year of Maximum Value at Bottom Mat
25	0.02	40	0.03	35
30	0.03	45	0.06	40
35	0.04	50	0.09	40
40	0.06	55	0.15	45
45	0.07	60	0.22	50
50	0.09	65	0.31	55

Table 4-4: Maximum Chloride Concentrations for a 3.0-in. OCD with a Surface Treatment

Treatment Year	Maximum Chloride Concentration after Treatment at Top Mat (lb Cl ⁻ /yd ³ Concrete)	Year of Maximum Value at Top Mat	Maximum Chloride Concentration after Treatment at Bottom Mat (lb Cl ⁻ /yd ³ Concrete)	Year of Maximum Value at Bottom Mat
25	0.01	40	0.01	35
30	0.02	45	0.03	40
35	0.03	50	0.05	45
40	0.04	55	0.07	50
45	0.05	60	0.11	50
50	0.06	65	0.16	55

**Table 4-5: Maximum Chloride Concentrations for a 2.0-in. OCD
without a Surface Treatment**

Treatment Year	Maximum Chloride Concentration after Treatment at Top Mat (lb Cl ⁻ /yd ³ Concrete)	Year of Maximum Value at Top Mat	Maximum Chloride Concentration after Treatment at Bottom Mat (lb Cl ⁻ /yd ³ Concrete)	Year of Maximum Value at Bottom Mat	Year Chloride Concentration at Top Mat \geq 2.0 lb Cl ⁻ /yd ³ Concrete
25	15.21	75	0.66	75	35
30	14.68	75	0.50	75	40
35	13.97	75	0.37	75	45
40	13.01	75	0.32	45	50
45	11.84	75	0.44	50	55
50	10.34	75	0.58	55	60

**Table 4-6: Maximum Chloride Concentrations for a 2.5-in. OCD
without a Surface Treatment**

Treatment Year	Maximum Chloride Concentration after Treatment at Top Mat (lb Cl ⁻ /yd ³ Concrete)	Year of Maximum Value at Top Mat	Maximum Chloride Concentration after Treatment at Bottom Mat (lb Cl ⁻ /yd ³ Concrete)	Year of Maximum Value at Bottom Mat	Year Chloride Concentration at Top Mat \geq 2.0 lb Cl ⁻ /yd ³ Concrete
25	11.83	75	0.29	75	40
30	11.03	75	0.21	75	45
35	10.09	75	0.15	75	50
40	8.95	75	0.15	45	55
45	7.53	75	0.22	50	60
50	5.77	75	0.31	55	65

nearest 5 years, as the exact deck ages at which either the maximum chloride concentrations were reached or the chloride concentrations exceeded the threshold value were not calculated.

Tables 4-2, 4-3, and 4-4 show the results for a bridge deck with an applied surface treatment for OCD values of 2.0, 2.5, and 3.0 in., respectively. The results indicate that, when a

**Table 4-7: Maximum Chloride Concentrations for a 3.0-in. OCD
without a Surface Treatment**

Treatment Year	Maximum Chloride Concentration after Treatment at Top Mat (lb Cl ⁻ /yd ³ Concrete)	Year of Maximum Value at Top Mat	Maximum Chloride Concentration after Treatment at Bottom Mat (lb Cl ⁻ /yd ³ Concrete)	Year of Maximum Value at Bottom Mat	Year Chloride Concentration at Top Mat \geq 2.0 lb Cl ⁻ /yd ³ Concrete
25	9.28	75	0.13	75	45
30	8.37	75	0.09	75	50
35	7.32	75	0.06	75	55
40	6.13	75	0.07	50	60
45	4.82	75	0.11	50	65
50	3.62	75	0.16	55	70

surface treatment is used, the concentration at either the top or bottom mat of reinforcing steel does not reach or exceed 2.0 lb of chloride per cubic yard of concrete after hydrodemolition during the 75 years of simulated bridge deck service life. With a majority of the original chloride ions being removed during the hydrodemolition process and with a surface treatment preventing further chloride ion ingress after hydrodemolition, changes in the chloride concentration over time are caused by upward and downward diffusion of the chloride ions that remain in the original concrete substrate. Due to their closer proximity to the bottom mat of reinforcing steel, the chloride ions reach maximum values at the bottom mat 5 to 10 years before they reach maximum values at the top mat, and the maximum values at the bottom mat are generally at least twice as high as the maximum values at the top mat.

Tables 4-5, 4-6, and 4-7 show the results for a bridge deck without an applied surface treatment for OCD values of 2.0, 2.5, and 3.0 in., respectively. The results indicate that, when a surface treatment is not used, the chloride concentration at the top mat of reinforcing steel exceeds 2.0 lb of chloride per cubic yard of concrete within 10, 15, and 20 years for OCD values

of 2.0, 2.5, and 3.0 in., respectively. Although a majority of the original chloride ions are removed during the hydrodemolition process, the absence of a surface treatment allows further chloride ion ingress after hydrodemolition. Therefore, changes in chloride concentration over time are caused not only by upward and downward diffusion of the chloride ions that remain in the original concrete substrate, but also by chloride ingress that results from the application of deicing salts. The results of the numerical modeling clearly suggest that a surface treatment should be applied as part of the rehabilitation process to seal the deck against further chloride ingress; although the results indicate that the chloride concentration at the bottom mat of reinforcing steel does not reach or exceed 2.0 lb of chloride per cubic yard of concrete during the 75 years of simulated bridge deck service life, the top mat of reinforcing steel will experience chloride-induced corrosion beginning 10 to 20 years after rehabilitation without an applied surface treatment.

4.4 Blow-through Analysis

The numerical experiments performed to investigate factors that influence the occurrence of blow-throughs in concrete bridge decks when hydrodemolition is used generated results in terms of the main effect of each input variable on the occurrence of blow-throughs and interactions among selected input variables. In addition, the blow-through analysis was applied to two bridge decks in northern Utah that were rehabilitated using hydrodemolition. For each analysis, blow-through can be expected when the calculated factor of safety is less than 1.0, but a minimum factor of safety of 3.0, as commonly specified in engineering practice, is desired to guard against blow-through.

Regarding the main effects of each input variable on the occurrence of blow-throughs, Table 4-8 lists the range, interval, and average for each input parameter that was varied in the experimentation. The parameters include transverse rebar spacing, concrete compressive strength, depth of removal below the bottom of the top reinforcing mat, orifice size, water pressure, and jet angle. The parameters that were held constant include reinforcing bar size, longitudinal rebar spacing, and concrete type. Specifically, based on typical UDOT practice, a No. 5 reinforcing bar size was assumed, the longitudinal rebar spacing was set at 12 in., and normal concrete, as opposed to lightweight concrete, was specified.

The main effects are presented in Figures 4-5 to 4-10, in which a dashed horizontal line marks a factor of safety of 3.0. The factor of safety significantly increases with increasing values of transverse rebar spacing and concrete compressive strength and decreasing values of depth of removal below the bottom of the top reinforcing mat, orifice size, and water pressure within the ranges of these parameters investigated in this experimentation. The factor of safety is relatively insensitive to jet angle. While a factor of safety less than 1.0 did not occur in these analyses of main effects, a factor of safety less than 3.0 occurred for an orifice size of 0.25 in., which supports the observation by some questionnaire survey respondents who indicated that an orifice

Table 4-8: Ranges of Parameters for Evaluation of Main Effects in Blow-Through Analysis

Statistic	Transverse Rebar Spacing (in.)	Concrete Compressive Strength (psi)	Depth of Removal below Bottom of Top Reinforcing Mat (in.)	Orifice Size (in.)	Water Pressure (ksi)	Jet Angle (degrees)
Range	6-12	2,000-8,000	0.25-1.25	0.10, 0.25	10-40	0-20
Interval	1	1,000	0.25	NA	5	5
Average	9	5,000	0.75	0.10	25	10

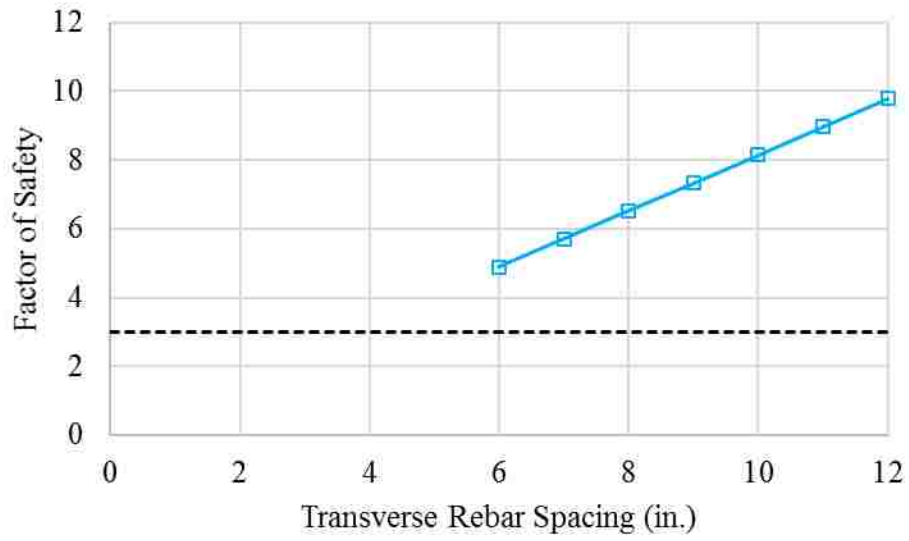


Figure 4-5: Main effect of transverse rebar spacing.

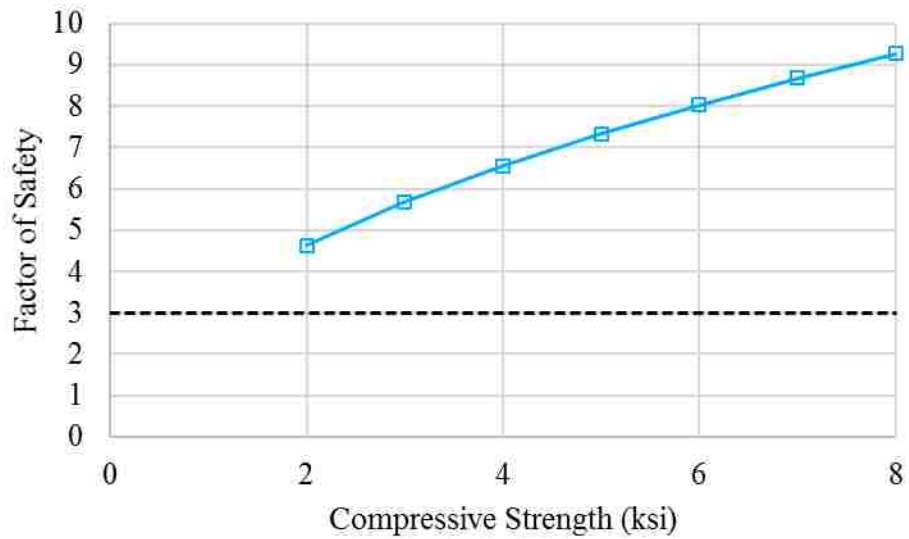


Figure 4-6: Main effect of concrete compressive strength.

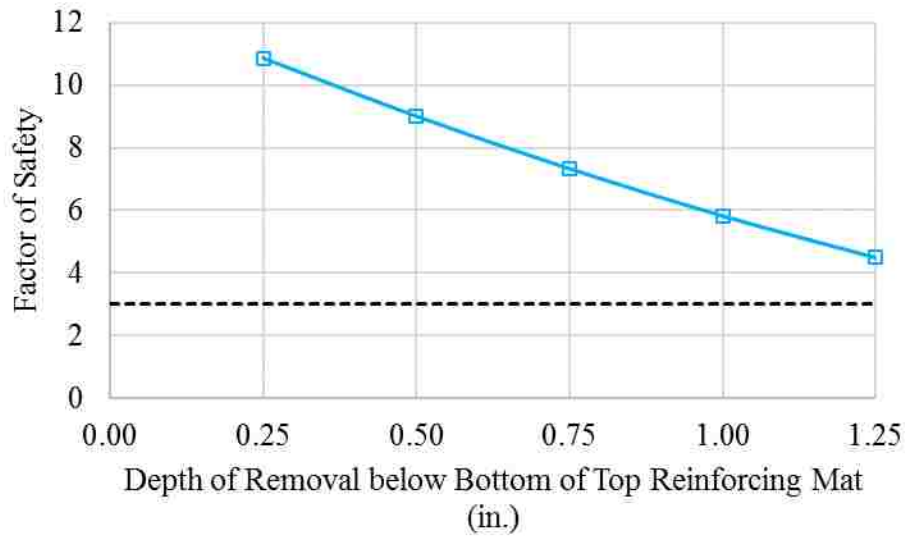


Figure 4-7: Main effect of depth of removal below bottom of top reinforcing mat.

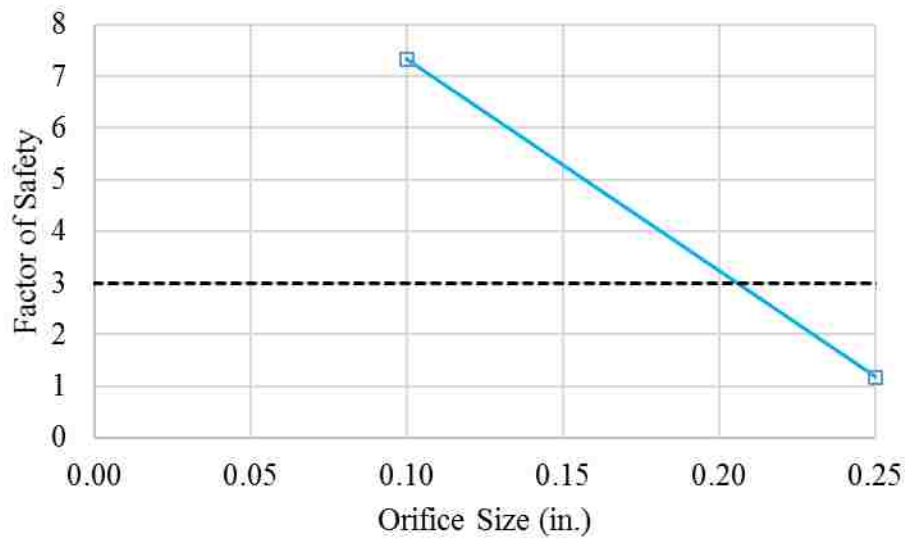


Figure 4-8: Main effect of orifice size.

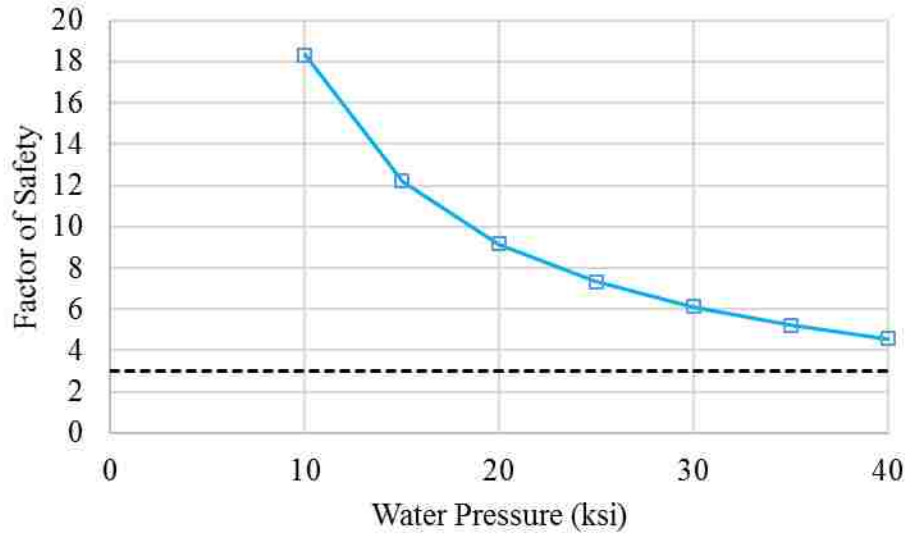


Figure 4-9: Main effect of water pressure.

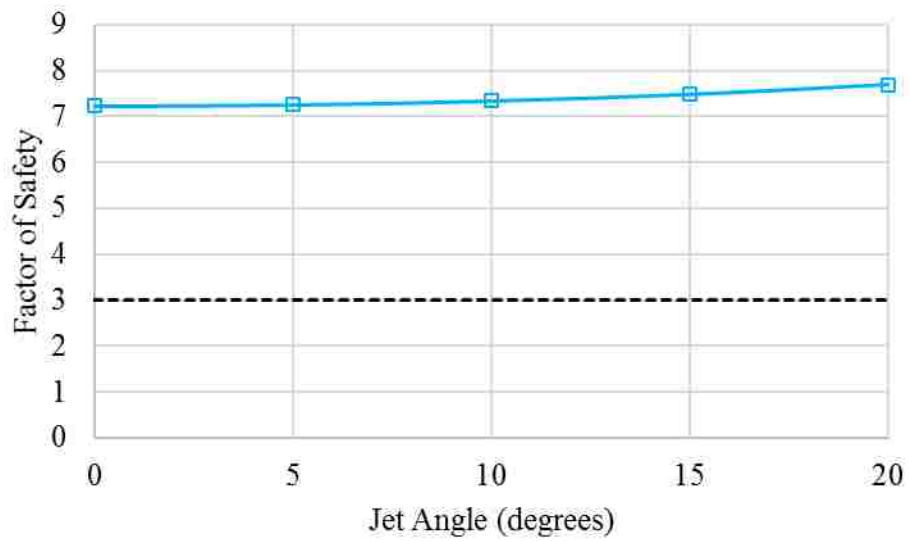


Figure 4-10: Main effect of jet angle.

size of 0.25 in. is inappropriate for hydrodemolition of concrete bridge decks because the greater force exerted by the high-pressure water jets with a larger orifice size increases the likelihood of blow-throughs. In all cases, the governing mode of failure for each parameter investigated in the experiment was the bending moment in the orientation where the length of the concrete beam is greater than the width of the concrete beam.

Regarding the interactions among selected input variables, Table 4-9 lists the range and interval for each input parameter that was varied in the experimentation. The parameters include transverse rebar spacing, concrete compressive strength, and water pressure. The parameters that were held constant include reinforcing bar size, longitudinal rebar spacing, concrete type, depth of removal below the bottom of the top reinforcing mat, orifice size, and jet angle. Specifically, based on typical UDOT practice, a No. 5 reinforcing bar size was assumed, the longitudinal rebar spacing was set at 12 in., normal concrete was specified, the depth of removal below the bottom of the top reinforcing mat was set at 0.75 in., the orifice size was set at 0.10 in., and the jet angle was set at 10 degrees. As previously stated, a depth of removal of 0.75 in. below the top reinforcing mat corresponds to a remaining concrete thickness above the bottom reinforcing mat of 2.0 in. The orifice size was held constant at 0.10 in. because that was the orifice size used by the majority of the survey respondents, and the results of the earlier experimentation (in terms of the main effect of each input variable) support selection of this value for minimizing the

Table 4-9: Ranges of Parameters for Evaluation of Interactions in Blow-Through Analysis

Statistic	Transverse Rebar Spacing (in.)	Concrete Compressive Strength (psi)	Water Pressure (ksi)
Range	6-12	2,000-8,000	10-40
Interval	2	2,000	10

occurrence of blow-through. A jet angle of 10 degrees with respect to the vertical axis of the nozzle was selected as an average value for most hydrodemolition projects.

The interactions are presented in Figures 4-11 to 4-14, in which a dashed horizontal line again marks a factor of safety of 3.0. While a factor of safety less than 1.0 did not occur in these analyses of interactions, a factor of safety less than 3.0 occurred for four combinations of the input parameters. The specific values of transverse rebar spacing, concrete compressive strength, and water pressure in those combinations are presented in Table 4-10. The values typically represent low transverse rebar spacing, low concrete compressive strength, and high water pressure. These combinations, and equivalent combinations not explicitly analyzed, should be avoided in practice to minimize the occurrence of blow-through during hydrodemolition. Furthermore, because the analysis performed in this research does not directly account for the

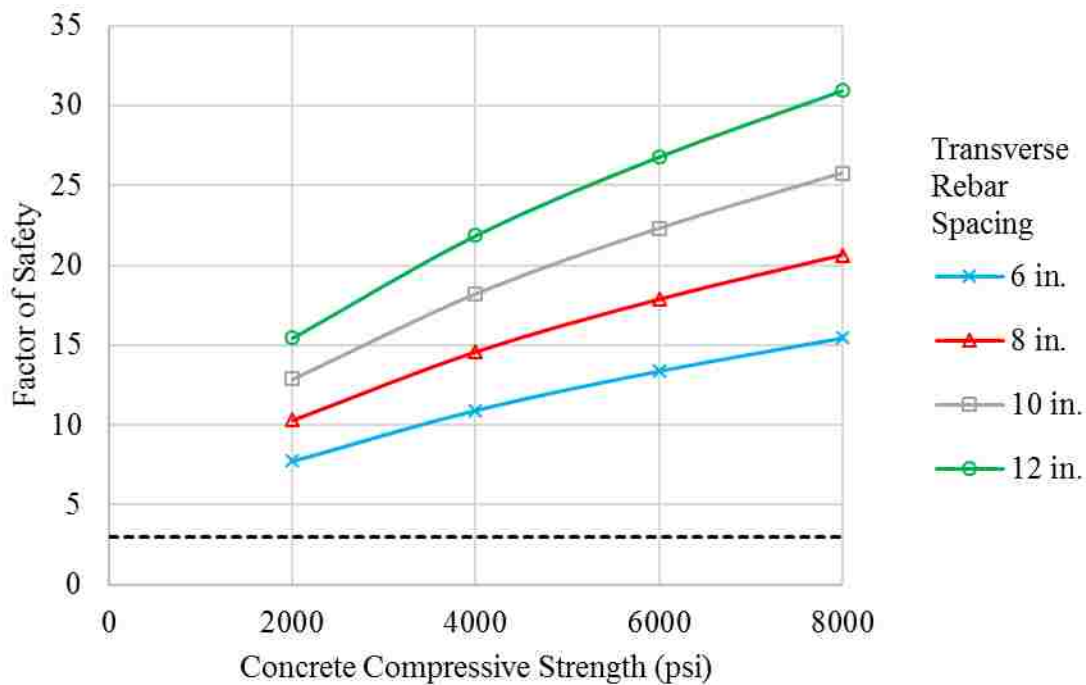


Figure 4-11: Interaction between concrete compressive strength and transverse rebar spacing for water pressure of 10 ksi.

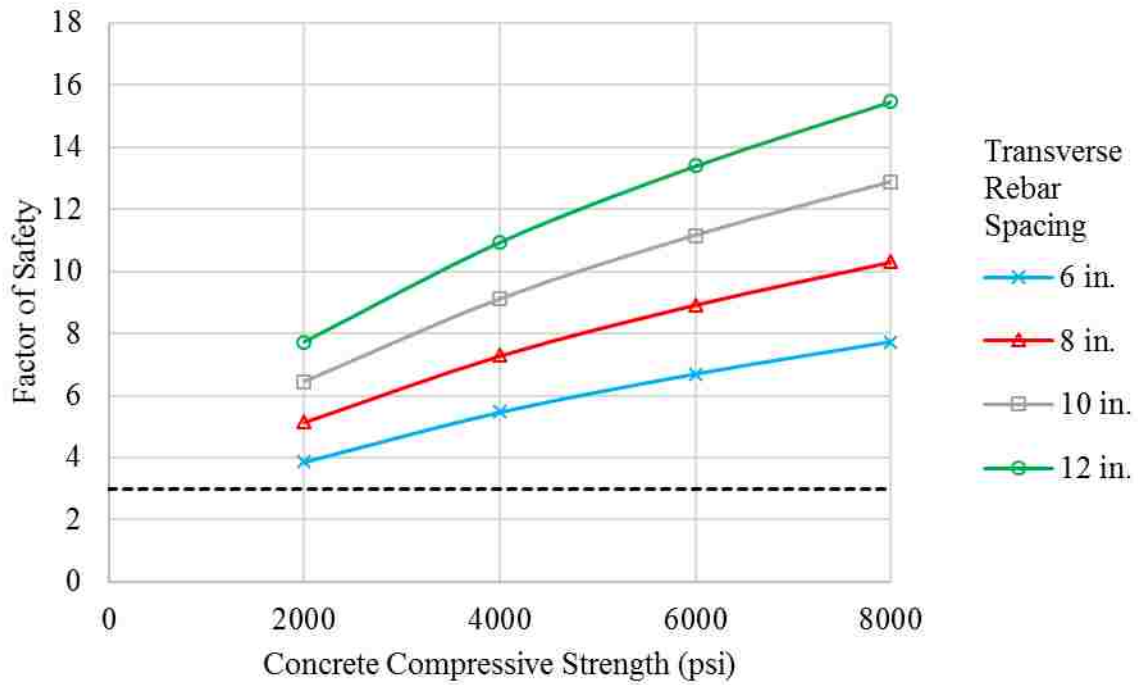


Figure 4-12: Interaction between concrete compressive strength and transverse rebar spacing for water pressure of 20 ksi.

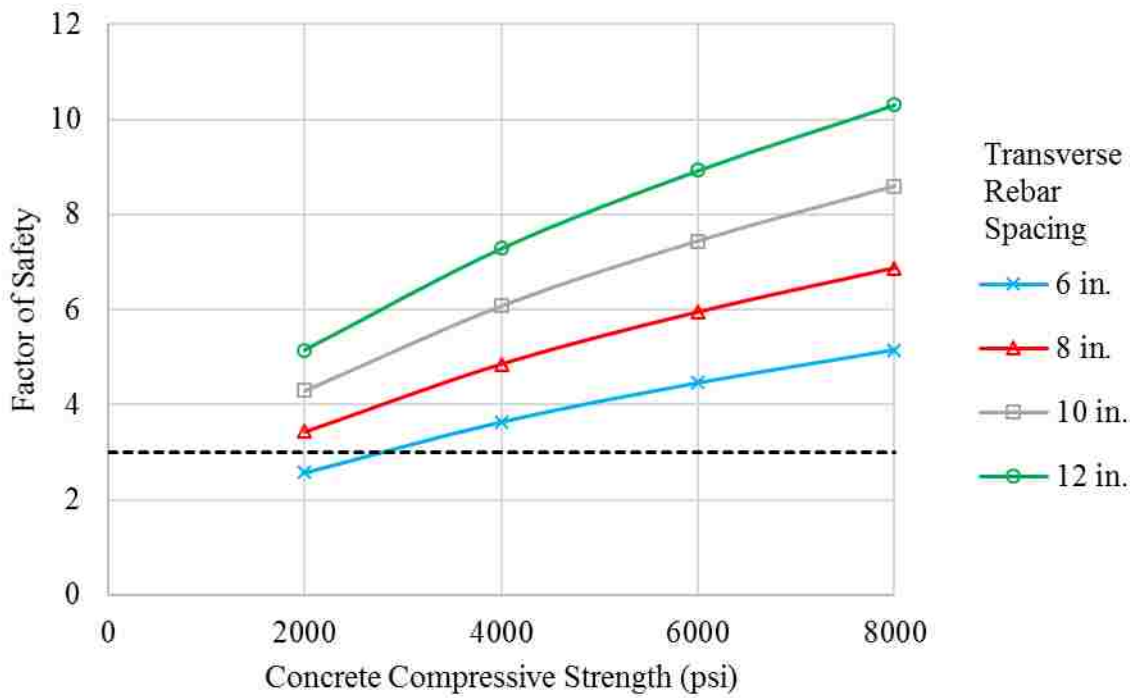


Figure 4-13: Interaction between concrete compressive strength and transverse rebar spacing for water pressure of 30 ksi.

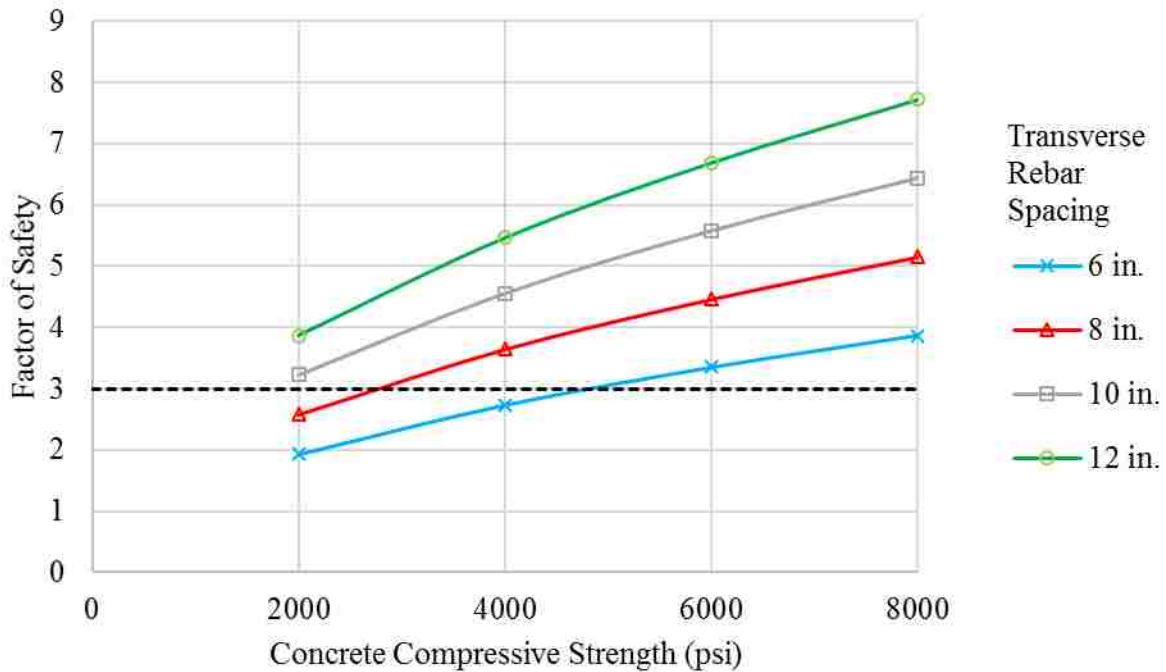


Figure 4-14: Interaction between concrete compressive strength and transverse rebar spacing for water pressure of 40 ksi.

Table 4-10: Parameter Combinations with Factor of Safety Less Than 3.0

Combination	Transverse Rebar Spacing (in.)	Concrete Compressive Strength (psi)	Water Pressure (ksi)	Factor of Safety
1	6	2,000	30	2.58
2	6	2,000	40	1.96
3	8	2,000	40	2.58
4	6	4,000	40	2.73

possibility of cracking in concrete bridge decks, the actual factors of safety may be considerably lower in all cases than those calculated and reported in Figures 4-5 to 4-14. In all cases, the governing mode of failure for each parameter investigated in the experiment was the bending moment in the orientation where the length of the concrete beam is greater than the width of the concrete beam.

Application of the blow-through analysis to two case studies on bridge decks in northern Utah that were rehabilitated using hydrodemolition generated results for a number of actual “worst-case” scenarios for both bridge decks. In the analyses, the total removal depth was calculated as the sum of the OCD for the top mat, the diameter of the transverse bar in the top mat, the diameter of the longitudinal bar in the top mat, and the specified depth of removal below the top mat. In addition, the height of the concrete beam was calculated as the difference between the deck thickness and the sum of the total removal depth, the 1.0-in. OCD for the bottom mat specified for both decks, the diameter of the transverse bar in the bottom mat, and half the diameter of the longitudinal bar in the bottom mat.

The extent of blow-through that occurred during hydrodemolition of the bridge deck investigated for case study #1 is shown in Figure 4-15, in which the areas that experienced blow-through are outlined. The blow-throughs were concentrated in areas between girders where the bottom of the deck was unsupported. Analysis showed that approximately 10.8 percent of the total bridge deck area experienced blow-through during hydrodemolition, which is a significant amount considering that the total bridge deck area is large at 40,613 ft². An example of the extensive blow-through damage on the bridge deck in case study #1, photographed after hydrodemolition, is shown in Figure 4-16.

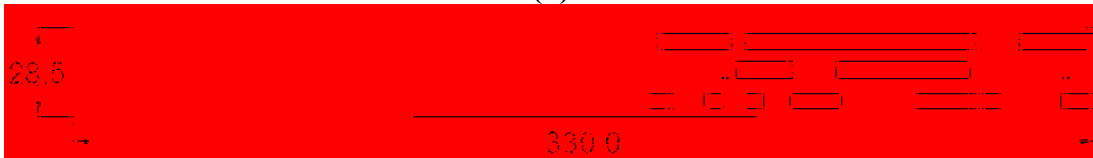
For case study #1, the values of several input parameters needed to perform a blow-through analysis of this bridge deck were determined. The original bridge deck had a thickness of 7.5 in. (Guthrie et al. 2014). The OCD for the top mat of reinforcing steel was 2.0 in., while the OCD for the bottom mat of reinforcing steel was 1.0 in. For the transverse reinforcement, No. 4 and No. 5 bars were used in both the top and bottom mats. For the longitudinal reinforcement, No. 9 and No. 10 bars were used in the top mat, and No. 5 bar was used in the bottom mat. The



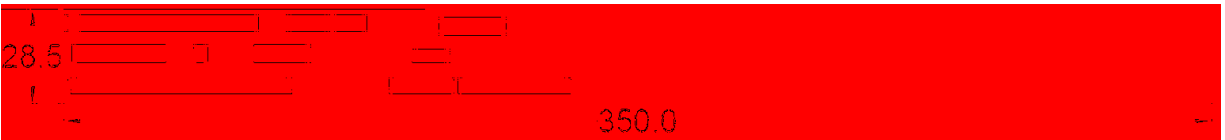
(a)



(b)



(c)



(d)

Figure 4-15: Blow-through map for case study #1: (a) 0-350 ft, (b) 350-745 ft, (c) 745-1,075 ft, and (d) 1,075-1,425 ft.



Figure 4-16: Significant blow-through of the deck in case study #1.

longitudinal reinforcement spacing generally varied from 10 to 12 in., while the transverse reinforcement spacing generally varied from 4 to 7 in.; the longitudinal reinforcement spacing was held constant at 12 in. in the analyses. The deck was constructed using normal concrete. The actual concrete compressive strength at the time of hydrodemolition was estimated to vary from 2,000 to 4,000 psi. The depth of concrete removal below the top mat of reinforcing steel was estimated to vary from 0.50 to 1.00 in. An oscillating nozzle was used, and the orifice size was 0.10 in. The water pressure for this project was 20,000 psi, and the jet angle was held constant at 10 degrees with respect to the vertical axis of the nozzle.

As shown in Table 4-11, nine scenarios were analyzed for case study #1 to evaluate the potential for the occurrence of blow-through. For all nine scenarios, the governing mode of failure is the bending moment in the orientation where the length of the concrete beam is greater than the width of the concrete beam. Five of the nine scenarios resulted in a factor of safety less than 1.0. Efflorescence on the bottom of the deck as shown in Figure 4-17, the blow-through analysis developed in this research correctly predicted a high potential for blow-through on this deck.

The extent of blow-through that occurred during hydrodemolition of the bridge deck investigated for case study #2 is shown in Figure 4-18, in which the areas that experienced blow-through are outlined. Analysis showed that less than 1.0 percent of the total bridge deck area experienced blow-through during hydrodemolition, which is an insignificant amount considering that the total bridge deck area is 5,210 ft². An example of the minimal blow-through damage on the bridge deck in case study #2, photographed after hydrodemolition, is shown in Figure 4-19.

For case study #2, the values of several input parameters needed to perform a blow-through analysis of this bridge deck were determined. The original bridge deck had a thickness of 8.5 in. The OCD for the top mat of reinforcing steel was 2.0 in., while the OCD for the bottom

Table 4-11: Blow-through Analysis Results for Various Scenarios for Case Study #1

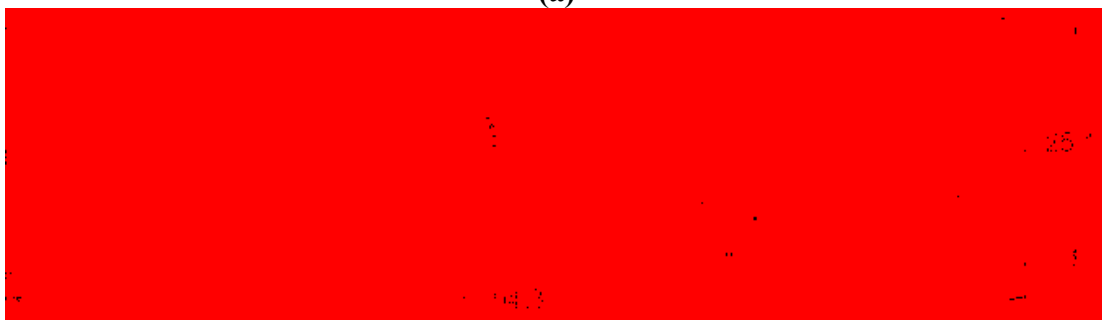
Input Parameter	Scenario									
	1	2	3	4	5	6	7	8	9	10
Top Longitudinal Reinforcing Bar Size	No. 10	No. 10	No. 10	No. 10	No. 10	No. 10	No. 8	No. 8	No. 8	No. 8
Top Transverse Reinforcing Bar Size	No. 4	No. 4	No. 4	No. 4	No. 4	No. 4	No. 3	No. 3	No. 3	No. 4
Bottom Longitudinal Reinforcing Bar Size	No. 7	No. 8	No. 8	No. 7	No. 7	No. 8	No. 7	No. 7	No. 7	No. 7
Bottom Transverse Reinforcing Bar Size	No. 4	No. 4	No. 4	No. 4	No. 4	No. 4	No. 3	No. 3	No. 3	No. 4
Assumed Concrete Reinforcing Bar Spacing (in.)	4	4	4	4	4	4	4	4	4	4
Concrete Compressive Strength (psi)	4000	4000	4000	4000	4000	4000	4000	4000	4000	4000
Reinforced Depth Ratio (L _o /L _u)	0.72	0.72	0.72	0.72	1.22	1.00	1.00	1.00	1.00	1.00
Minimum Factor of Safety	1.40	0.92	1.01	1.27	0.50	1.00	1.11	0.95	0.90	0.90
Predicted Blow-through	No	Yes	No	Yes	Yes	No	Yes	Yes	Yes	Yes



Figure 4-17: Significant efflorescence and cracking on the underside of the deck in case study #1.



(a)



(b)

Figure 4-18: Blow-through map for case study #2: (a) 0-104.2 ft and (b) 104.2-208.5 ft.



Figure 4-19: Insignificant blow-through of the deck in case study #2.

mat of reinforcing steel was 1.0 in. For the transverse reinforcement, No. 5 bars were used in both the top and bottom mats. For the longitudinal reinforcement, No. 7 bars were used in the top mat, and No. 5 and No. 7 bars were used in the bottom mat. The longitudinal reinforcement spacing generally varied from 10 to 12 in., while the transverse reinforcement spacing generally varied from 4 to 6 in.; the longitudinal reinforcement spacing was held constant at 12 in. in the analyses. The deck was constructed using normal concrete. The actual concrete compressive strength at the time of hydrodemolition was estimated to vary from 2,000 to 4,000 psi. The depth of concrete removal below the top mat of reinforcing steel was estimated to vary from 0.50 to 1.00 in. A rotating nozzle was used, and the orifice size was 0.10 in. The water pressure for this project was 34,000 psi, and the jet angle was held constant at 10 degrees with respect to the vertical axis of the nozzle.

As shown in Table 4-12, nine scenarios were analyzed for case study #2 to evaluate the potential for the occurrence of blow-through. For all nine scenarios, the governing mode of failure is the bending moment in the orientation where the length of the concrete beam is greater

Table 4-12: Blow-through Analysis Results for Various Scenarios for Case Study #2

Input Parameter	Scenario								
	1	2	3	4	5	6	7	8	9
Top Longitudinal Reinforcing Bar Size	№11	№11	№11	№11	№11	№11	№11	№11	№11
Top Transverse Reinforcing Bar Size	№8	№8	№8	№8	№8	№8	№8	№8	№8
Bottom Longitudinal Reinforcing Bar Size	№11	№11	№11	№11	№11	№11	№11	№11	№11
Bottom Transverse Reinforcing Bar Size	№8	№8	№8	№8	№8	№8	№8	№8	№8
Assumed concrete Relat. Spalling (%)	0	0	4	4	7	7	8	9	9
Concrete Compressive strength (psi)	4000	4000	4000	4000	4000	4000	4000	4000	4000
Reinforced Equiv. Relat. Top Longitudinal Bar Size	№11	№11	№11	№11	№11	№11	№11	№11	№11
Reinforced Equiv. Relat. Bottom Longitudinal Bar Size	№11	№11	№11	№11	№11	№11	№11	№11	№11
Predicted Blow-through	Yes	No	No	No	No	Yes	No	No	No

than the width of the concrete beam. Although eight of the nine scenarios resulted in a factor of safety less than 3.0, none of the scenarios resulted in a factor of safety less than 1.0. Therefore, although the factors of safety may have actually been lower, due to minor cracking on the bottom of the deck as shown in Figure 4-20, the blow-through analysis developed in this research correctly predicted a low potential for blow-through on this deck.



Figure 4-20: Insignificant efflorescence and cracking on the underside of the deck in case study #2.

4.5 Summary

This chapter presents the results of the questionnaire survey, chloride concentration analysis, and blow-through analysis performed in this research. Regarding the questionnaire survey conducted to assess current practices of selected hydrodemolition companies, while some respondents indicated that certain parameters vary, depending on the project, the survey responses are valuable for understanding typical practices and were used to design the numerical experiments performed to investigate factors that influence the occurrence of blow-throughs in

concrete bridge decks when hydrodemolition is used. All survey participants reported that blow-throughs are a common occurrence when using hydrodemolition on concrete bridge decks. A few mentioned that blow-throughs are most common on bridge decks with efflorescence on the underside of the deck, which is usually an indication that the deck has experienced extensive cracking and may have high chloride concentrations.

The numerical modeling performed to investigate the effects of hydrodemolition treatment timing on chloride concentration profiles in concrete bridge decks for depths of concrete removal below the top mat of reinforcing steel generated chloride concentration profiles through a 75-year service life given a specific OCD, treatment time, and surface treatment usage. The results indicate that, when a surface treatment is used, the concentration at either the top or bottom mat of reinforcing steel does not reach or exceed 2.0 lb of chloride per cubic yard of concrete after hydrodemolition during the 75 years of simulated bridge deck service life. The results also indicate that, when a surface treatment is not used, the chloride concentration at the top mat of reinforcement exceeds 2.0 lb of chloride per cubic yard of concrete within 10, 15, and 20 years for OCD values of 2.0, 2.5, and 3.0 in., respectively.

The numerical experiments performed to investigate factors that influence the occurrence of blow-throughs in concrete bridge decks when hydrodemolition is used generated results in terms of the main effect of each input variable on the occurrence of blow-throughs and interactions among selected input variables. In addition, the blow-through analysis was applied to two bridge decks in northern Utah that were rehabilitated using hydrodemolition. For each analysis, blow-through can be expected when the calculated factor of safety is less than 1.0, but a minimum factor of safety of 3.0, as commonly specified in engineering practice, is desired to guard against blow-through. The factor of safety significantly increases with increasing values of

transverse rebar spacing and concrete compressive strength and decreasing values of depth of removal below the bottom of the top reinforcing mat, orifice size, and water pressure within the ranges of these parameters investigated in this experimentation. The factor of safety is relatively insensitive to jet angle. While a factor of safety less than 1.0 did not occur in the analyses of interactions, a factor of safety less than 3.0 occurred for four combinations of the input parameters. These combinations, and equivalent combinations not explicitly analyzed, should be avoided in practice to minimize the occurrence of blow-through during hydrodemolition.

Application of the blow-through analysis to two case studies on bridge decks in northern Utah that were rehabilitated using hydrodemolition generated results for a number of actual “worst-case” scenarios for both bridge decks. Nine scenarios were analyzed for each case study to evaluate the potential for the occurrence of blow-through. For case study #1, five of the nine scenarios resulted in a factor of safety less than 1.0, and all of the scenarios resulted in a factor of safety less than 3.0. Given that approximately 10.8 percent of the total bridge deck area experienced blow-through during hydrodemolition, the blow-through analysis developed in this research correctly predicted a high potential for blow-through on this deck. For case study #2, eight of the nine scenarios resulted in a factor of safety less than 3.0, but none of the scenarios resulted in a factor of safety less than 1.0. Given that less than 1.0 percent of the total bridge deck area experienced blow-through during hydrodemolition, the blow-through analysis developed in this research correctly predicted a low potential for blow-through on this deck.

5 CONCLUSION

5.1 Summary

The objectives of this research were 1) to investigate the effects of hydrodemolition treatment timing on chloride concentration profiles in concrete bridge decks for depths of concrete removal below the top mat of reinforcing steel and 2) to investigate factors that influence the occurrence of blow-throughs in concrete bridge decks when hydrodemolition is used. The objectives of this research were met by conducting a questionnaire survey of hydrodemolition companies, performing numerical modeling of chloride concentration to investigate hydrodemolition treatment timing on typical Utah bridge decks, and using structural analysis to investigate factors that influence the occurrence of blow-throughs during hydrodemolition.

A questionnaire survey was conducted by telephone and email to assess current practices of selected hydrodemolition companies that rehabilitate concrete bridge decks throughout the country. The survey findings were used to design the numerical experiments performed to investigate factors that influence the occurrence of blow-throughs in concrete bridge decks when hydrodemolition is used. A total of five survey participants, who were typically the managers of the hydrodemolition companies, responded to the survey, and their answers were compiled to assess the current bridge deck rehabilitation practices of these hydrodemolition companies.

Numerical modeling was performed to investigate the effects of hydrodemolition treatment timing on chloride concentration profiles in concrete bridge decks for depths of

concrete removal below the top mat of reinforcing steel. Based on communications with UDOT engineers to determine current practice, appropriate ranges of removal and overlay depths were selected for use in the modeling process. Crossing the various levels of the experimental factors in a full-factorial structure generated a total of 36 unique combinations, or scenarios. Modeling of the decks without treatment was performed first to develop a baseline chloride concentration profile to which the chloride concentration profiles for various treatment times were compared. Modeling was then performed for each unique combination of OCD, treatment time, and surface treatment application to produce chloride concentration profiles that would be expected after hydrodemolition and rehabilitation were performed. The latest timing of rehabilitation that maintained a chloride concentration level below 2.0 lb of chloride per cubic yard of concrete at the levels of both the top and bottom mats of reinforcing steel was identified for each unique combination of OCD and surface treatment application.

For this research, a spreadsheet was developed to investigate six modes of failure, or blow-through, that can potentially be experienced by a concrete bridge deck during hydrodemolition. These modes of failure include bending, one-way shear, and two-way shear, each of which is analyzed in both the orientation where the length is greater than the width and in the orientation where the length is smaller than the width. For any of these failure modes, if the capacity of the concrete deck section is less than the forces applied by the high-pressure water jets, blow-through can be expected. The factor of safety against blow-through is calculated as the shear or moment capacity of the concrete section divided by the shear force or moment imparted by the high-pressure water jets. Several calculations were required in the analysis of the simulated concrete beam, including those for modulus of rupture, moment of inertia, maximum moment, cracking moment, maximum shear force, one-way shear strength, and two-way shear

strength. The bridge deck parameters that were used as inputs in the blow-through analysis are bridge deck thickness, OCD, reinforcing bar size, longitudinal rebar spacing, transverse rebar spacing, type of concrete, concrete compressive strength, and removal depth. The hydrodemolition equipment parameters that were used as inputs in the blow-through analysis are orifice size, water pressure, and angle of jet. Following development of the spreadsheet, numerical experiments were performed to investigate factors that influence the occurrence of blow-throughs in concrete bridge decks when hydrodemolition is used. Finally, the blow-through analysis was applied to two case studies on bridge decks in northern Utah that were rehabilitated using hydrodemolition.

5.2 Findings

While some survey respondents indicated that certain parameters vary, depending on the project, the responses are valuable for understanding typical practices and were used to design the numerical experiments performed to investigate factors that influence the occurrence of blow-throughs in concrete bridge decks when hydrodemolition is used. All survey participants reported that blow-throughs are a common occurrence when using hydrodemolition on concrete bridge decks. A few mentioned that blow-throughs are most common on bridge decks with efflorescence on the underside of the deck, which is usually an indication that the deck has experienced extensive cracking and may have high chloride concentrations.

The numerical modeling performed to investigate the effects of hydrodemolition treatment timing on chloride concentration profiles in concrete bridge decks for depths of concrete removal below the top mat of reinforcing steel generated chloride concentration profiles through a 75-year service life given a specific OCD, treatment time, and surface treatment usage.

The results indicate that, when a surface treatment is used, the concentration at either the top or bottom mat of reinforcing steel does not reach or exceed 2.0 lb of chloride per cubic yard of concrete after hydrodemolition during the 75 years of simulated bridge deck service life. The results also indicate that, when a surface treatment is not used, the chloride concentration at the top mat of reinforcement exceeds 2.0 lb of chloride per cubic yard of concrete within 10, 15, and 20 years for OCD values of 2.0, 2.5, and 3.0 in., respectively.

The numerical experiments performed to investigate factors that influence the occurrence of blow-throughs in concrete bridge decks when hydrodemolition is used generated results in terms of the main effect of each input variable on the occurrence of blow-throughs and interactions among selected input variables. In addition, the blow-through analysis was applied to two bridge decks in northern Utah that were rehabilitated using hydrodemolition. For each analysis, blow-through can be expected when the calculated factor of safety is less than 1.0, but a minimum factor of safety of 3.0, as commonly specified in engineering practice, is desired to guard against blow-through. The factor of safety significantly increases with increasing values of transverse rebar spacing and concrete compressive strength and decreasing values of depth of removal below the bottom of the top reinforcing mat, orifice size, and water pressure within the ranges of these parameters investigated in this experimentation. The factor of safety is relatively insensitive to jet angle. While a factor of safety less than 1.0 did not occur in the analyses of interactions, a factor of safety less than 3.0 occurred for four combinations of the input parameters. These combinations, and equivalent combinations not explicitly analyzed, should be avoided in practice to minimize the occurrence of blow-through during hydrodemolition.

Application of the blow-through analysis to two case studies on bridge decks in northern Utah that were rehabilitated using hydrodemolition generated results for a number of actual

“worst-case” scenarios for both bridge decks. Nine scenarios were analyzed for each case study to evaluate the potential for the occurrence of blow-through. For case study #1, five of the nine scenarios resulted in a factor of safety less than 1.0, and all of the scenarios resulted in a factor of safety less than 3.0. Given that approximately 10.8 percent of the total bridge deck area experienced blow-through during hydrodemolition, the blow-through analysis developed in this research correctly predicted a high potential for blow-through on this deck. For case study #2, eight of the nine scenarios resulted in a factor of safety less than 3.0, but none of the scenarios resulted in a factor of safety less than 1.0. Given that less than 1.0 percent of the total bridge deck area experienced blow-through during hydrodemolition, the blow-through analysis developed in this research correctly predicted a low potential for blow-through on this deck.

5.3 Recommendations

Hydrodemolition should be considered as an effective means of removing chloride-contaminated concrete from immediately around and even below the top mat of reinforcing steel and allowing mechanical interlock with the new concrete placed after hydrodemolition. For bridge decks typical of those in Utah, treatment times from 25 to at least 50 years can be specified to achieve significant extensions in deck service life. To maximize deck service life, a surface treatment should be applied to seal the rehabilitated concrete deck against further chloride ingress.

The blow-through analysis developed in this research has potential for use as a tool for determining if bridge decks that are no longer suitable for repair using traditional concrete removal techniques may still be good candidates for repair using hydrodemolition. As the blow-through analysis assumes that the concrete within the simulated beam is intact, without cracking

or other distresses, the resulting calculations should be supplemented with visual inspection of the deck; extensive cracking and efflorescence on the bottom of the deck may indicate a higher probability of blow-through during hydrodemolition.

REFERENCES

- Arora, P., Popov, B. N., Haran, B., Ramasubramanian, M., Popva, S., and White, R. E. (1997). "Corrosion initiation time of steel reinforcement in a chloride environment: A one dimensional solution." *Elsevier J. Corros Sci*, 39(4), 739-759.
- Basheer, L., Cleland, D. J., and Long, A. E. (1998). "Protection provided by surface treatments against chloride induced corrosion." *Springer J. Mat. and Struct.*, 31(211), 459-464.
- Bentz, D. P. (2007). "Prediction of a chloride ion penetration profile for a concrete." <<http://ciks.cbt.nist.gov/~bentz/clpen2.html>> (June 1, 2016).
- Birdsall, A. W., Guthrie, W. S., and Bentz, D. P. (2007). "Effects of initial surface treatment timing on chloride concentrations in concrete bridge decks." *Transportation Research Record*, 2028, 103-110.
- Clark, G. L., and Hawley, G. G. (1966). *The encyclopedia of chemistry*, Reinhold Publishing Corporation, New York, NY.
- Federal Highway Administration (FHWA). (2011). *Bridge preservation guide*, Publication Number FHWA-HIF-11042, Washington, DC.
- Freeze, R., and Cheery, J. (1979). *Groundwater*, Prentice Hall, NJ.
- Gere, J. M., and Goodno, B. J. (2013). *Mechanics of materials*, Eighth Edition, Cengage Learning, Stamford, CT.
- Grace, N., Hanson, J., and AbdelMessih, H. (2004). *Inspection and deterioration of bridge decks constructed using stay-in-place metal forms and epoxy-coated reinforcement*, Research Report R, Michigan Department of Transportation, Lansing, MI.
- Guthrie, W. S., Nolan, C. D., and Bentz, D. P. (2008). "Effect of initial scarification and overlay treatment timing on chloride concentrations in concrete bridge decks." *Transportation Research Record*, 2220, 66-74.
- Guthrie, W. S., Flannery, D. L., Baxter, J. S., and Mazzeo, B. A. (2014). *Demonstration of vertical impedance and acoustic impact-echo testing for condition assessment of a concrete bridge deck with a concrete overlay and polymer surface treatment*, Research Report, Utah Department of Transportation, Salt Lake City, UT.

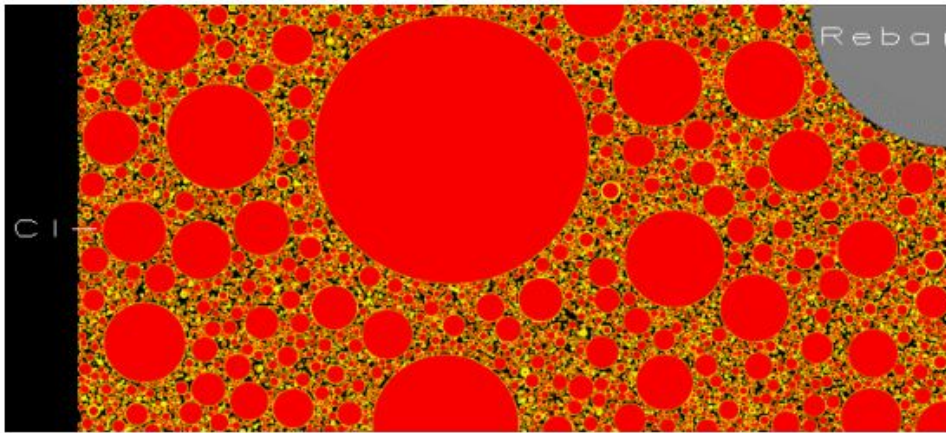
- Guthrie, W. S., Frost, S. L., Birdsall, A. W., Linford, E. T., Ross, L. A., Crane, R. A., and Eggett, D. L. (2006). "Effect of stay-in-place metal forms on performance of concrete bridge decks." *Transportation Research Record*, 1958, 33-41.
- Guthrie, W. S., Nelsen, T., and Ross, L. A. (2005). *Performance of concrete bridge deck surface treatments*, Report No. UT-05.05, Utah Department of Transportation, Salt Lake City, UT.
- Harries, K., McCabe, M., and Sweriduk, M. (2013). *Structural evaluation of slab rehabilitation by method of hydrodemolition and latex modified overlay*, Report No. FHWA-PA-2013-006-PIT WO 01, Pennsylvania Department of Transportation, Harrisburg, PA.
- Hema, J., Guthrie, W. S., and Fonseca, F. (2004). *Concrete bridge deck condition assessment and improvement strategies*, Report No. UT-04.16, Utah Department of Transportation, Salt Lake City, UT.
- Hopwood, T., Goff, C., Wells, D., and Palle, S. (2015). *Hydrodemolition and use of a rapid early strength latex modified concrete overlay*, Report No. KTC-TA-15-01/KHIT6-15-1F, Kentucky Transportation Cabinet, Flemingsbury, KY.
- International Concrete Repair Institute (ICRI). (2014). *Guide for the preparation of concrete surfaces for repair using hydrodemolition methods*, Guideline No. 310.3R-2014, Rosemont, IL.
- Lees, T. P. (1992). "Deterioration mechanisms." *Durability of concrete structures*, G. Mays, ed., E & FN SPON, London, UK.
- Lewis, R. J. (2001). *Hawley's condensed chemical dictionary*, Fourteenth Edition, John Wiley and Sons, Inc., New York, NY.
- Mays, G. (1992). *Durability of concrete structures*, E & FN SPON, London, UK.
- McCormac, J. C., and Brown, R. H. (2015). *Design of reinforced concrete*, Tenth Edition, Wiley, New York, NY.
- Mindess, S., Young, J. F., and Darwin, D. (2003). *Concrete*, Second Edition, Prentice Hall, NJ.
- Momber, A. W. (2005). *Hydrodemolition of concrete surfaces and reinforced concrete structures*, Aachen University, Aachen, Germany.
- Pan, X., Shi, Z., Shi, C., Ling, T., and Li, N. (2016). "A review of concrete surface treatment Part 1: types and mechanisms." *Elsevier J. Constr. Bldg. Mat.*, 132(1), 578-590.
- Patnaik, A., and Baah, P. (2015). *Cracking behavior of structural slab bridge decks*, Report No. FHWA/OH-2015/4, Ohio Department of Transportation, Columbus, OH.

- Poulsen, E., and Mejlbro, E. (2006). *Diffusion of chloride in concrete: Theory and application*, Taylor and Francis, Inc., New York, NY.
- Suryavanshi, A. K., Swamy, R. N., and McHugh, S. (1998). "Chloride penetration into reinforced concrete slabs." *Canadian J. of Civ. Eng.*, 25(1), 87-95.
- Swamy, R. N., and Tanikawa, S. (1993). "An external surface coating to protect concrete and steel from aggressive environments." *Springer J. Mat. and Struct.*, 26(162), 465-478.
- Wenzlick, J. D. (2002). *Hydrodemolition and repair of bridge decks*, Report No. RDTO2-002, Missouri Department of Transportation, Jefferson City, MO.
- Weyers, R. E., Prowell, B. D., Sprinkel, M. M., and Vorster, M. (1993). *Concrete bridge protection, repair, and rehabilitation relative to reinforcement corrosion: A methods application manual*, Report No. SHRP-S-360, Strategic Highway Research Program, Washington, DC.
- Zhang, J. Z., McLoughlin, I. M., and Buenfield, N. R. (1998). "Modeling of chloride diffusion into surface-treated concrete." *Elsevier J. Cem. Concr. Comp.*, 20(4), 253-261.

APPENDIX A SAMPLE INPUTS FOR CHLORIDE CONCENTRATION ANALYSIS

Figure A-1 contains screenshots showing the inputs used while performing the numerical modeling. The inputs for the time of treatment, length of experiment (total duration of exposure), member thickness, depth of reinforcement, time of surface treatment application, time at which hydrodemolition (milling and filling) was performed, depth of concrete removal (milling), and thickness of new (filling) concrete were changed to reflect the parameters of each specific experiment. All other inputs were held constant, as depicted.

Prediction of a Chloride Ion Penetration Profile for a Concrete



Prediction is based on a one-dimensional finite difference solution of Fick's second law of diffusion, with a variable external chloride concentration and a two-layer representation of the concrete. Surface treatment option has been added in 2006 and mill and fill option added in 2007 in collaboration with Prof. Guthrie of Brigham Young University.

Please supply the following parameters (defaults provided)

Environmental Parameters

Specify external chloride concentration and temperature as a function of month of the year:

Month	Ext. chloride conc. (moles/liter)	Temperature (°C)
January	4.273	-2.278
February	3.865	1.167
March	3.326	5.444
April	2.800	9.833
May	2.429	14.889

Figure A-1: Inputs used for numerical modeling program.

2/23/2017

Chloride Penetration Simulation Including Mill and Fill

June	<input type="text" value="2.311"/>	<input type="text" value="20.611"/>
July	<input type="text" value="2.479"/>	<input type="text" value="25.500"/>
August	<input type="text" value="2.887"/>	<input type="text" value="24.222"/>
September	<input type="text" value="3.427"/>	<input type="text" value="18.444"/>
October	<input type="text" value="3.952"/>	<input type="text" value="11.778"/>
November	<input type="text" value="4.324"/>	<input type="text" value="4.889"/>
December	<input type="text" value="4.441"/>	<input type="text" value="-1.278"/>

Beginning month of exposure is:

Total duration of exposure days

Unexposed boundary condition is

Structural Design Parameters

Member thickness m

Depth of Reinforcement mm

Concrete Mixture Parameters

w/c ratio

Degree of hydration

Volume fraction of aggregate %

Air content %

Initial chloride concentration of concrete g chloride/g cement [Guidance](#)

Diffusion Coefficients (D) of Original Concrete

Click [here](#) to view database of concrete diffusivities from literature.

<https://concrete.nist.gov/clpenmillandfill.html>

2/5

Figure A-1: Continued.

Note that all diffusion coefficients are apparent diffusivity values, as we are modelling transport in the pore space of the concrete based on Fick's 2nd law.

Time dependent diffusion coefficient for bulk concrete takes the form of $D=D_{inf}+D_i*t^{-m}$

Be sure that you use values of m in the range (0,1).

Reference: Mangat and Molloy, Materials and Structures, Vol. 27, 338-346, 1994. Note- Mangat and Molloy found m values ranging from 0.44 to 0.86 and also that approximately:

$$m=2.5(w/c)-0.6$$

To have a constant D value with time, simply set D_{inf} to this desired value and D_i to zero

D_{inf} m*m/s at 25 C

D_i m*m/s

m

Curing time before exposure of concrete to chlorides days (Recommended > 0)

The surface layer of the concrete may have a different (lower or higher) D value than the bulk concrete due to carbonation or poor curing practices. Input the surface layer D value relative to the bulk D value and the thickness of this layer. To bypass this feature, set the skin layer thickness to 0.0 or use $D(\text{surface concrete})/D(\text{bulk concrete})=1.0$.

Ratio D (surface concrete)/D (bulk concrete)

Thickness of surface layer mm

Activation Energy for diffusion kJ/mole

Chloride Binding Parameters [Guidance](#)

Based on a Langmuir isotherm of the form:
 $C(\text{bound})=(\alpha*C(\text{free}))/(1.+\beta*C(\text{free}))$

where C(bound) is in (mole Cl⁻)/kg cement and
 C(free) is in (mole Cl⁻)/L

Alpha

Beta

Rate constant for binding s⁻¹

Chloride Reaction Parameters [Guidance](#)

Assuming the formation of Freidel's salt from all of the
 C_3A and C_4AF initially available in the cement powder.

Figure A-1: Continued.

C₃A content of cement % on a mass basis

C₄AF content of cement % on a mass basis

Rate constant for aluminate reactions with chloride s⁻¹

New Feature (March 2006)

Allows application of a surface treatment at a specific time, beyond which further transfer of chlorides into/out of the top surface is prohibited.

Set this time to a time greater than the total exposure time to turn off this feature

Time at which surface treatment is applied days

Mill and Fill Concrete Options (February 2007)

Time at which milling and filling is performed days

Depth of milling m

Thickness of new (filling) concrete m

w/c ratio of new concrete

Degree of hydration of new concrete

Volume fraction of aggregate for new concrete %

Air content of new concrete %

Initial chloride concentration of new concrete g chloride/g cement [Guidance](#)

Diffusion Coefficients (D) of New Concrete

Time dependent diffusion coefficient for bulk concrete takes the form of $D=D_{inf}+D_i*t^{-m}$

Be sure that you use values of m in the range (0,1).

To have a constant D value with time, simply set D_{inf} to this desired value and D_i to zero

D_{inf} m²/s at 25 C

D_i m²/s

m

Curing time before exposure of new concrete to external chlorides days (Recommended > 0)

Figure A-1: Continued.

2/23/2017

Chloride Penetration Simulation Including Mill and Fill

The surface layer of the concrete may have a different (lower or higher) D value than the bulk concrete due to carbonation or poor curing practices. Input the surface layer D value relative to the bulk D value and the thickness of this layer. To bypass this feature, set the skin layer thickness to 0.0 or use $D(\text{surface concrete})/D(\text{bulk concrete})=1.0$.

Ratio $D(\text{surface concrete})/D(\text{bulk concrete})$

Thickness of surface layer mm

Figure A-1: Continued.

APPENDIX B BLOW-THROUGH ANALYSIS FOR CASE STUDY #1

Figures B-1 and B-2 show the sections of the bridge plans that were used to determine identifiers for the bar sizes used for the blow-through analyses for case study #1. Figures B-3 and B-4 show the bridge plans that were used to determine which bar sizes were used as transverse reinforcement and longitudinal reinforcement, respectively. Figures B-5 through B-13 show the blow-through analysis outputs for each of the nine scenarios that were analyzed for case study #1.

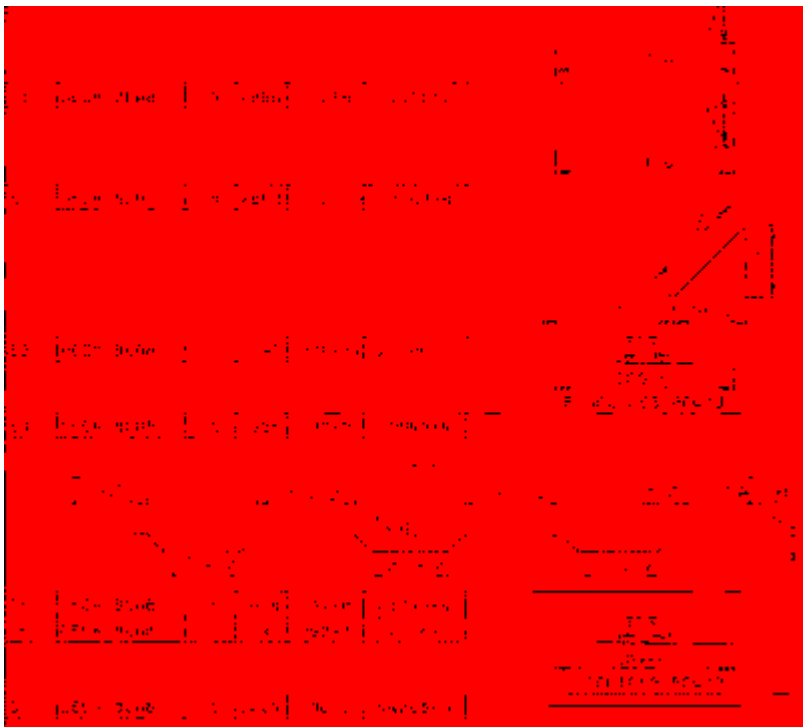


Figure B-1: First set of reinforcement plans for bridge deck in case study #1.

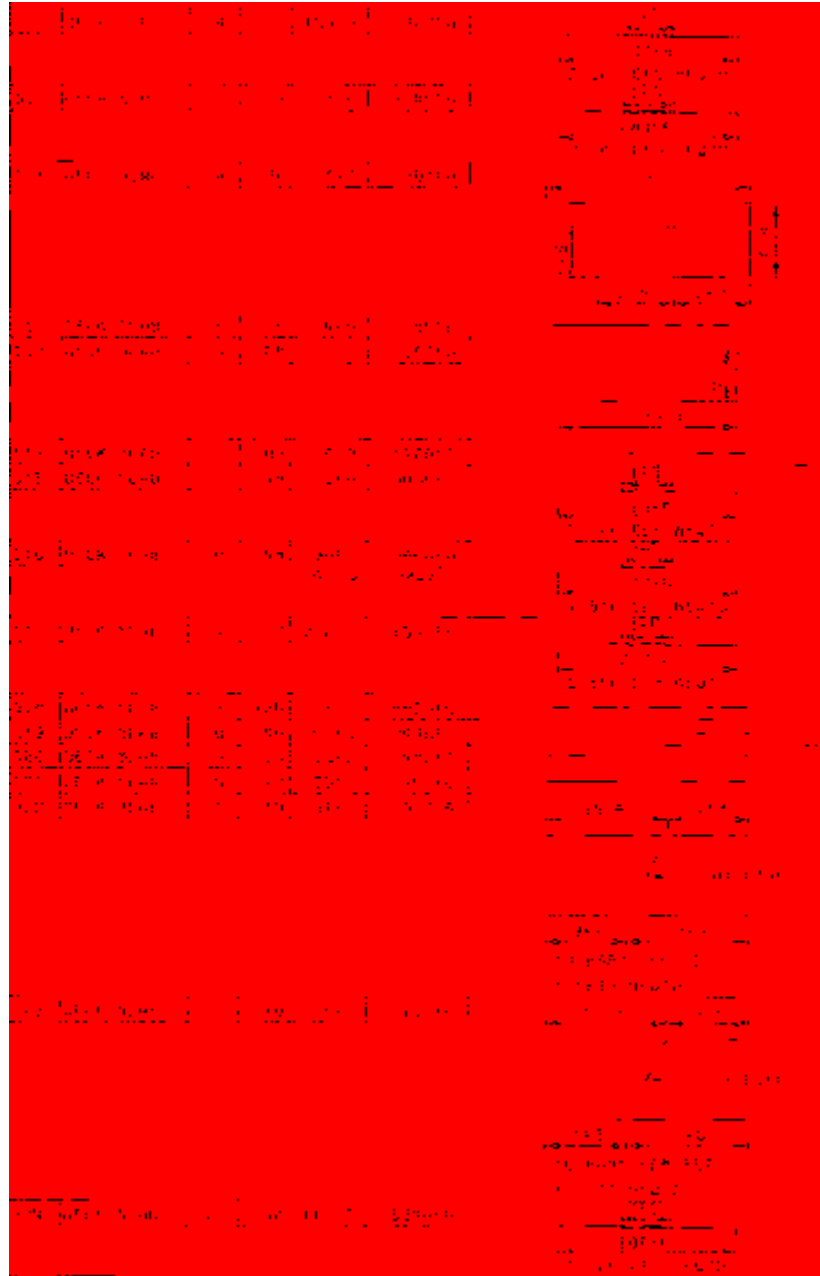


Figure B-2: Second set of reinforcement plans for bridge deck in case study #1.



Figure B-3: Bridge schematic showing transverse reinforcing bar locations for bridge deck in case study #1.



Figure B-4: Bridge schematic showing longitudinal reinforcing bar locations for bridge deck in case study #1.

A B C D E F G H I J K L M N O P Q R S T U V W X Y Z	Depth to Top Reinforcing Bar (D _{top})	23.5 in
	Reinforcing Bar Size	5
	Dist. Between	7.5 in
	Depth to Bottom Reinforcing Bar	1 in
	Depth of Concrete Slab (D _{slab})	31.5 in
	Thickness of Slab (h)	7
	Width of Slab (b)	1
	Number of Columns	100
	Slab Area (A _{slab})	100
	Angle of Slab (α)	90 deg
	Beam Load (P)	10
	Design Compression Strength (F _{cd})	100
	Effective Slab and Column Width	
	Area of Slab (A _{slab})	
	Concrete Strength Class (or Section Modulus) (M _{cr})	100
	Length (L)	10
	Case (a)	1
	Height (H)	
	Concrete Class	
	Aggregate Material	
	Modulus of Elasticity (E _c)	3,600,000 psi
	Type of Span	one-way
	Support of Slab (a, b)	0.60 in
Effective length (l _e)	1.10 in	
Distance to Slab (a _{slab})	0.55 in	
Design Moment (M _u)	100 ft-kip	
Cracking Moment (M _{cr})	8.5 ft-kip	
Cracking Moment (M _{cr})		
Moment (M _u)	100 ft-kip	
One-Way Slab Strength of Concrete (M _u)	200 ft-kip	
Failure in One-Way Slab		
One-Way Slab Strength of Concrete (M _u)	177 ft-kip	
Failure in Two-Way Slab		
Moment (M _u)	100 ft-kip	
Cracking Moment (M _{cr})	100 ft-kip	
Cracking Moment (M _{cr})		
Moment (M _u)	77 ft-kip	
One-Way Slab Strength of Concrete (M _u)	170 ft-kip	
Failure in One-Way Slab		
One-Way Slab Strength of Concrete (M _u)	170 ft-kip	
Failure in One-Way Slab		

Figure B-5: Blow-through analysis for scenario 1 of case study #1.

Depth to Top Reinforcing Mat (D _T)	2.0 m
Reinforcing Mat Height	0
Deck Thickness	1.5 m
Depth to Bottom Reinforcing Mat (D _B)	8
Depth of Concrete Reinforcement (Depth to Bottom Mat)	3.075 m
Width of Deck	0
Height of Pier (H _P)	6.5
Pier Diameter	0
Angle of Lead (θ)	0 deg
Pier Length (L _P)	6
Concrete Compressive Strength (f _{ck})	60 MPa
Reinforcing Steel Yield Strength (f _{yk})	0
Average Concrete Modulus of Elasticity (E _c)	0
Compressive Strength Based on Reinforcing Steel Yield Strength	0 MPa
Length (l)	0
Factor (k)	0
Factor (l)	0
Concrete Type	0
Aggregate Shape Factor	0
Modulus of Elasticity (E)	47.1 GPa
Tips of Pier	one-way
Modulus of Inertia (I _c)	0.53 m ⁴
Modulus of Inertia (I _{sc})	6.24 m ⁴
Distance to Neutral Axis (h)	0.75 m
Modulus of Inertia (I _{sc})	49.08 m ⁴
Effective Moment (M _{eff})	14.1 kNm
Cracking Due to Flexure (M _{cr})	0.26 kNm
Maximum Shear (V _{max})	0.26 kN
Concrete Shear Strength of Concrete (V _{cr})	4.32 kN
Failure in One-Way Slab	0
Reinforcing Steel Strength of Concrete (V _{cr})	0.78 kN
Failure in Punching Shear (M _{cr})	0.149 kNm
Modulus of Inertia (I _c)	0.60 m ⁴
Cracking Due to Flexure (M _{cr})	0.26 kNm
Modulus of Inertia (I _c)	0.77 m ⁴
Concrete Shear Strength of Concrete (V _{cr})	0.76 kN
Failure in One-Way Slab	0
Reinforcing Steel Strength of Concrete (V _{cr})	0.24 kN
Failure in Punching Shear (M _{cr})	0

Figure B-6: Blow-through analysis for scenario 2 of case study #1.

Depth to Top Reinforcing Bar (in)	17.5
Reinforcing Bar Size	#5
Depth to Bottom Reinforcing Bar (in)	7.5
Depth to Bottom Reinforcing Bar	6 in
Depth to Center of Reinforcing Bar (in)	12.5
Number of Bar Passes	1
Width of Slab (in)	1
Modulus of Elasticity (ksi)	29,000
Reinforcing Bar Modulus (ksi)	29,000
Angle of Load (deg)	45
Reinforcing Bar Yield Strength (ksi)	60
Design Compressive Strength of Concrete (ksi)	4,000
Concrete Reinforcing Steel Institute (C.R.S.I.)	
Average Deflection Reinforcing Bar (in)	
Compressive Strength Based on Concrete Modulus of Elasticity (ksi)	4,000
Length (ft)	10
Depth (ft)	10
Height (ft)	10
Concrete Type	
Aggregate Modulus (ksi)	
Modulus of Elasticity (ksi)	13,000
Type of Slab	One-Way Slab
Moment of Inertia (in ⁴)	116.7
Moment of Inertia (in ⁴)	12.19
Deflection (in) based on Area (in ²)	0.523
Maximum Moment (ft-k)	124.08
Cracking Moment (ft-k)	14.7
Cracking Deflection (in)	
Maximum Shear (kips)	27.35
One-Way Slab Strength of Concrete (psi)	6,410
Factor of One-Way Slab	
Flexure Shear Strength of Concrete (psi)	1,020
Factor of Flexure Shear	
Maximum Moment (ft-k)	124.08
Cracking Moment (ft-k)	14.7
Cracking Deflection (in)	
Maximum Shear (kips)	27.35
One-Way Slab Strength of Concrete (psi)	6,410
Factor of One-Way Slab	
Flexure Shear Strength of Concrete (psi)	1,020
Factor of Flexure Shear	

Figure B-7: Blow-through analysis for scenario 3 for case study #1.

Depth to Top Reinforcement from O.C.P.	2.17 in
Reinforcing Bar Size	#4
Block Thickness	7.5 in
Depth to Bottom Reinforcement	6 in
Condition of Concrete Removal	10.75 in
Number of Reinforcing Bars	1
Width of Plate	1
Number of Plates	1
Normal Diameter	1
Area of Concrete	36 sq ft
Plate Length	16
Design Compressive Strength f_{cm} of Schmidt Hammer Concrete	40
Average of 10 Hammer Readings	40
Compressive Strength Bars of an Schmidt Hammer Concrete	60
Length of Bar	16
Bar Size	#4
Height of Concrete	16
Concrete Type	
Aggregate Replaced	
Modulus of Elasticity E_c	3,541,458 psi
Type of Splice	lap splice
Moment of Inertia I_g	11,855 in ⁴
Moment of Inertia I_{cr}	7,157 in ⁴
Ultimate Flexural Capacity	1,071 ft-k
Maximum Moment M_{max}	461.06 ft-kip
Cracking Moment M_{cr}	154.11 ft-kip
Cracking Due to Flexure	Yes
Maximum Moment M_{max}	461.06 ft-kip
Cracking Due to Temperature and Shrinkage	Yes
Failure in Compression	Yes
Cracking Shear Strength of Concrete M_{cr}	154.11 ft-kip
Failure in Flexure	Yes
Failure in Punching Shear	Yes
Maximum Moment M_{max}	461.06 ft-kip
Cracking Moment M_{cr}	154.11 ft-kip
Cracking Due to Temperature and Shrinkage	Yes
Maximum Moment M_{max}	461.06 ft-kip
Cracking Shear Strength of Concrete M_{cr}	154.11 ft-kip
Failure in Flexure	Yes
Failure in Punching Shear	Yes

Figure B-8: Blow-through analysis for scenario 4 for case study #1.

Depth of Top Reinforcing Bar (D _{top})	210 mm
Reinforcing Bar Size	#5
Depth of the knee	750 mm
Depth of Bottom Bar for long Dir.	60 mm
Depth of Top Reinforcing Bar (D _{top})	210 mm
Number of Vertical Bars	4
Vertical Bar Size	#5
Number of Bars	4
Angle of Load (θ)	45°
Force Load (P)	0
Design Compression Strength (C _{design})	34
Reinforcing Bar and Anchor Available	100%
Concrete Strength Ratio (f _c /f _{ck})	1.0
Compressive Strength Based on Schmidt's Hammer Value (f _{cm})	34
Length (L)	0
Diase (d)	0
Height (h)	0
Concrete Load	0
Appropriate Rept. ref.	
Thickness of Concrete (t)	100 mm
Type of Span	one-way
Volume of concrete (V _c)	0.45 m ³
Mass of concrete (M _c)	36.27 m ³
Distance to the column (L ₁)	0.65 m
Volume of concrete (V _{c1})	0.42 m ³
Mass of concrete (M _{c1})	34.56 m ³
Cracking Due to flexure	0
Maximum Shear (V _{max})	0
One-Way Shear Strength of Concrete (V _{c1})	110 kN
Factor in One-Way Shear	1
Cracking Shear Strength of Concrete (V _{c2})	100 kN
Volume of concrete (V _c)	0.45 m ³
Mass of concrete (M _c)	36.27 m ³
Cracking Moment (M _{cr})	0 kN-m
Cracking Due to flexure	0
Maximum Shear (V _{max})	0 kN
One-Way Shear Strength of Concrete (V _{c1})	110 kN
Factor in One-Way Shear	1
Cracking Shear Strength of Concrete (V _{c2})	100 kN

Figure B-10: Blow-through analysis for scenario 6 for case study #1.

Depth of Top Reinforcement in Pier	1.0 in
Reinforcing Bar Size	5
Depth of Pier	2.5 in
Depth to Bottom Reinforcing Bar	6 in
Depth of Concrete Pier cap	1.75 in
Number of Pier Piers	1
Width of Pier	1
Flexion on Pier base	0
Shear on Pier base	0
Angle of Load (°)	45 deg
Concrete Strength	4
Reinforcing Bar Strength (ksi)	60
Submerged Pier and Spigot Contribution	
Average Submerged Pier and Spigot	
Compressive Strength (ksi) of Concrete Pier and Spigot	4
Length (ft)	0
Stress (ksi)	0
Weight (lb)	0
Concrete Type	
Aggregate Fraction	
Volume of Pier and Spigot	4.043 cu ft
Top of Pier	0.000 ft
Mean of Pier and Spigot	11.590 in ³
Mean of Pier and Spigot	28.070 in ³
Force due to Water Area (ft)	0.000 in
Moment about Pier and Spigot	436.188 in ³ -ft
Cracking Moment (ft-k)	3.000 ft-k
Cracking Due to Flexure	
Moment about Pier and Spigot	77.360 ft-k
Over and Under Strength of Concrete (ft-k)	504.00
Factor of Over and Under	
Over and Under Strength of Concrete (ft-k)	1018.00
Factor of Over and Under	
Cracking Moment (ft-k)	222.040 ft-k
Cracking Due to Flexure	
Moment about Pier and Spigot	171.780 ft-k
Over and Under Strength of Concrete (ft-k)	171.780 ft-k
Factor of Over and Under	
Over and Under Strength of Concrete (ft-k)	21.124
Factor of Over and Under	

Figure B-11: Blow-through analysis for scenario 7 for case study #1.

Quantity of Reinforcing Bars (RB)	37.2 in.
Reinforcing Bar Size	5
Max. L. Side Inset	7.5 in.
Depth to Bottom Reinforcing Bar	8 in.
Depth to Concrete Top of J	3.775 in.
Number of the Reinforcing Bar	1
Area of the Bar	0.31
Flange to Flange	104
Mounts Center to	0
Angle of Load (α)	30 deg
Pressure (p)	0
Design Concrete Strength (f_c)	30
Effective Reinforcing Bar Area ($A_{s,eff}$)	
Average Reinforcing Bar and Diameter	
Concrete Strength (based on Section Modulus Method) (f_c)	30
Length (h)	0
Base (B)	0
Height (h)	0
Concrete Type	
Aggregate Fraction	
Modulus of Elasticity (E)	4018.2 ksi
Depth of Embedment	0.000 in.
Volume of Concrete	0.50 in ³
Modulus of Elasticity	13.00 ksi
Ultimate Moment (M _{ult})	1.53 in-k
Moment at Failure (M _{fail})	161.03 in-k
Cracking Moment (M _{cr})	4.27 in-k
Crack Load (P _{crack})	
Maximum Strain (ε _{max})	0.000
Overway Shear Strength of Concrete (V _{sc})	6.94 lb
Failure Load for Shear	
Overway Shear Strength of Concrete (V _{sc})	1.33 lb
Failure Load for Shear	
Maximum Moment (M _{max})	20.04 in-k
Cracking Moment (M _{cr})	1.09 in-k
Cracking Load (P _{crack})	
Maximum Strain (ε _{max})	0.000
Overway Shear Strength of Concrete (V _{sc})	1.33 lb
Failure Load for Shear	
Overway Shear Strength of Concrete (V _{sc})	1.33 lb
Failure Load for Shear	

Figure B-13: Blow-through analysis for scenario 9 for case study #1.

APPENDIX C BLOW-THROUGH ANALYSIS FOR CASE STUDY #2

Figure C-1 shows the sections of the bridge plans that were used to determine identifiers for the bar sizes used for the blow-through analyses for case study #2. Figures C-2 and C-3 show the bridge plans that were used to determine which bar sizes were used as transverse reinforcement and longitudinal reinforcement. Figures C-4 through C-12 show the blow-through analysis outputs for each of the trials that were analyzed for case study #2.

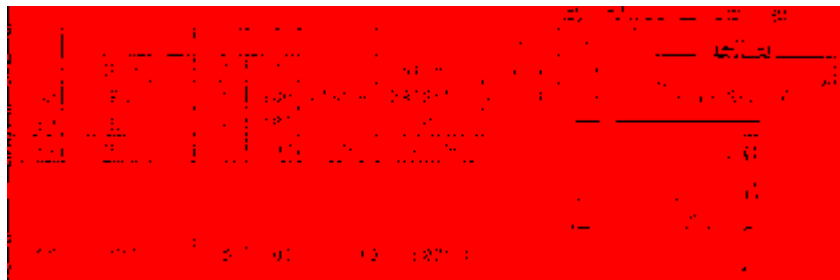


Figure C-1: Reinforcement plans for bridge deck in case study #2.

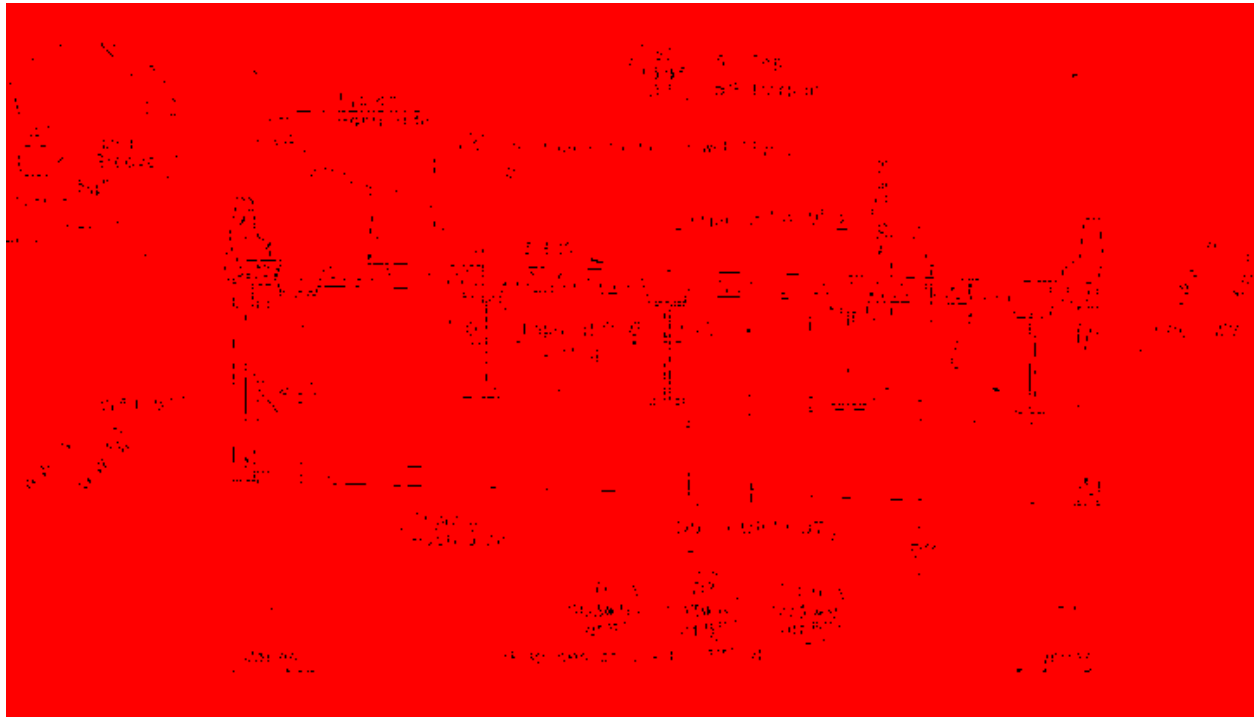


Figure C-2: Bridge schematic showing transverse reinforcing bar locations, deck thickness, and cover depths for bridge deck in case study #2.

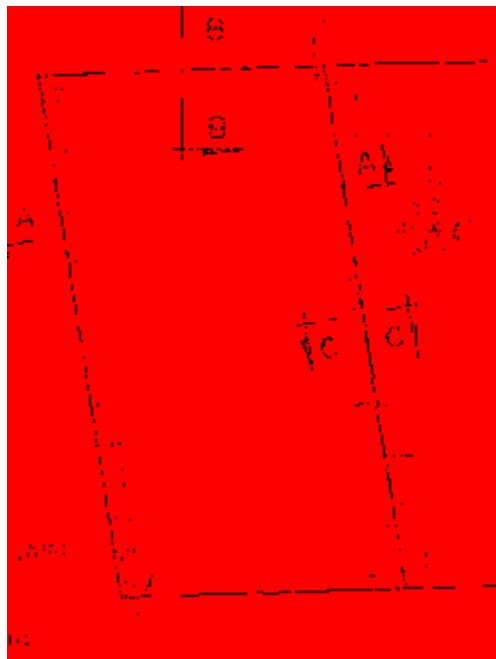


Figure C-3: Bridge schematic showing longitudinal reinforcing bar locations for bridge deck in case study #2.

Depth to Top Reinforcement from O.C.	2.17 m
Reinforcing Bar Size	#4
Block Thickness	0.5 m
Depth to Bottom Reinforcement	0 m
Condition of Concrete Removal	0.075 m
Number of Reinforcing Bars	1
Width of Plate	1 m
Number of Plywood	0 m
Normal Diameter	1
Area of Section	0.25 m ²
Plate Load Per	10
Design Compressive Strength (ϕP_n)	0.0
Schmid Factor and Number of Struts	
Average of Member Flexural Member	
Compressive Strength Bars of an Schmidt Member (ϕP_n)	0
Length of	1
Bar Area	1
Height of	1
Concrete Type	
Aggregate Replaced	
Modulus of Elasticity (E_c)	47.8 GPa
Type of Span	One-way
Moment of Inertia (I_g)	0.017 m ⁴
Moment of Inertia (I_{cr})	0.017 m ⁴
Ultimate Flexure Capacity	1.23 kN
Maximum Moment (M_{max})	155.84 kN-m
Cracking Due to Flexure	0.15 mm
Maximum Shear (V_{max})	11.07 kN
Shear due to Design Load (V_{design})	0.15 kN
Maximum Shear (V_{max})	11.07 kN
Cracking Shear Strength of Concrete (V_c)	100.1 kN
Failure of Punching Shear	
Moment of Inertia (I_{gross})	0.017 m ⁴
Cracking Moment (M_{cr})	0.15 kN-m
Cracking Due to Flexure	
Maximum Shear (V_{max})	11.07 kN
Ordering Shear Strength of Concrete (V_c)	100.1 kN
Failure of Punching Shear	
Punching Shear Strength of Concrete (V_c)	100.1 kN
Failure of Punching Shear	

Figure C-4: Blow-through analysis for scenario 1 for case study #2.

Design Parameters (Inputs)	Depth of Reinforcing Main (ft)	7.5	ft
	Reinforcing Bar Dia.	5	
	Depth of Layer	0.5	ft
	Depth of Custom Reinforcing Bar	2	ft
	Depth of Concrete Pier (ft)	3.17	ft
	Number of Jet Piers	1	
	Width Jet Pier	1	
	Diameter Pier cap	1.5	ft
	Height Diameter	1	ft
	Angle of Load (°)	30	deg
	Concrete Strength	4	ksi
	Design Compression Strength of $\phi_c P_n$	2.5	ksi
	Number of Pier Reinforcement Layers	2	
	Concrete Diameter Reinforcement Diameter	2	in
	Concrete Strength	4	ksi
	Concrete Type	1	
	Aggregate Percentage	1	
Design Results (Outputs)	Mechanical Friction (μ)	0.6	non-dimensional
	Load Factor	1.5	dimensionless
	Diameter of Jet Pier (ft)	5.00	ft
	Number of Jet Piers	2	
	Distance to Jet Pier (ft)	1.50	ft
	Moment Capacity (M_u)	399.94	in-kip
	Cracking Moment (M_{cr})	22.17	in-kip
	Cracking Due to Flexure	0	
	Maximum Shear (V_u)	7.46	kip
	One-Way Shear Strength of Concrete (V_c)	7.46	kip
	Failure in One-Way Shear	0	
	Punching Shear Strength of Concrete (V_p)	5.12	kip
	Failure in Punching Shear	0	
	Maximum Moment (M_u)	12.94	in-kip
	Cracking Moment (M_{cr})	7.07	in-kip
	Cracking Due to Flexure	0	
	Maximum Shear (V_u)	3.74	kip
One-Way Shear Strength of Concrete (V_c)	3.74	kip	
Failure in One-Way Shear	0		
Punching Shear Strength of Concrete (V_p)	3.74	kip	
Failure in Punching Shear	0		

Figure C-5: Blow-through analysis for scenario 2 for case study #2.

Depth of Top Reinforcing Bar (C/D)	2.0 in.
Area of Top Reinforcing Bar (A _s)	6
Depth of Bottom Reinforcing Bar (C/B)	U.S. in.
Area of Bottom Reinforcing Bar (A _s)	6
Depth of Concrete Pier (D)	3.175 in.
Length of the Pier (L)	1
Width of Pier (B)	1
Height of Pier (H)	1
Pier's Diameter	1
Angle of Load (α)	45°
Pier's Length	1
Design Concrete Compressive Strength (f _{cd})	4
Section Modulus for outer Available	
Average Section Modulus of Member	
Concrete Design Compressive Strength (f _{cd})	4
Length of Pier (L)	1
Pier's Width (B)	1
Pier's Height (H)	1
Concrete Load	
Aggregate Frictional	
Area of Pier (A _p)	3.175 in ²
Length of Pier (L)	1 in
Moment of Inertia (I _p)	3.94 in ⁴
Area of Pier (A _p)	3.175 in ²
Distance of Top of Pier (D _{top})	1.875 in.
Flexural Moment (M _u)	186.94 in-kb.
Cracking Moment (M _{cr})	107.7 in-kb.
Depth of Top to Fibers (D _{top})	1.875 in.
Moment Shear (M _u)	186.94 in-kb.
One-Way Shear Strength of Concrete (V _u)	186.94
Factor of One-Way Shear	
Punching Shear Strength of Concrete (V _u)	186.94
Factor of Punching Shear	
Flexural Moment (M _u)	186.94 in-kb.
Cracking Moment (M _{cr})	107.7 in-kb.
Cracking Load (k _{cr})	
Moment Shear (M _u)	186.94 in-kb.
One-Way Shear Strength of Concrete (V _u)	186.94
Factor of One-Way Shear	
Punching Shear Strength of Concrete (V _u)	186.94
Factor of Punching Shear	

Figure C-6: Blow-through analysis for scenario 3 for case study #2.

Depth to Top Reinforcing Bar (DCD)	1.11 m
Reinforcing Bar Size	#4
Deck Thickness	0.50 m
Depth to bottom Reinforcing Bar	0.61 m
Depth of Concrete Support	1.075 m
Number of Beams	1
Width of Beam	1
Nozzle Jet Pressure	68 MPa
Nozzle Diameter	0.025 m
Angle of Jet	45 deg
Stand-off (m)	0
Design Concrete strength (f'_c) (MPa)	30 MPa
Subgrade Retention Factor, R_{ret}	1
Average Subgrade Retention Factor	1
Compressive Strength of concrete (f'_c) (MPa) (assumed)	30 MPa
Length (L)	6 m
Depth (D)	0.6 m
Height (H)	0.6 m
Concrete type	normal weight
Aggregate fraction (F)	0.75
Modulus of Rupture (f_r)	1.46 MPa
Type of Span	one-way
Moment of inertia (I_g)	1.40 m ⁴
Moment of inertia (I_{cr})	0.25 m ⁴
Distance to Neutral Axis (d)	0.57 m
Moment of inertia (I_{eff})	0.94 m ⁴
Crack spacing (s_r)	84 mm
Cracking Due to Flexure	
Maximum Shear (V_{max})	21.49 kN
Crack Width due to flexure and concrete type	0.14 mm
Failure in One-Way Shear	
Flexure Capacity of Concrete (M_u)	1948 kN-m
Failure in Punching Shear	
Flexure Capacity (M_u)	221.75 kN-m
Cracking Due to Flexure	
Maximum Shear (V_{max})	12.49 kN
Crack Width due to flexure and concrete type	0.03 mm
Failure in One-Way Shear	
Flexure Capacity (M_u)	446.75 kN-m
Failure in Punching Shear	

Figure C-7: Blow-through analysis for scenario 4 for case study #2.

Depth of Corrosion at Top of CP	2.11 in
Reinforcing Bar Size	#4
Crack Width (in)	0.5 in
Depth of Distal Reinforcing Bar	6 in
Depth of Concrete Removal	0.75 in
Number of Reinforcing Bars	1
Number of Pre-stress	0
Normal Diameter	0
Angle of Verticality	30 deg
Reinforcing Bar	#6
Design Compressive Strength (f_{cr}) (ksi)	64
Reinforcing Bar Area (A_{br}) (in ²)	0.2
Average Compressive Strength (ksi)	64
Compressive Strength Bars (in Schmidt Number) (ksi)	64
Length (in)	0
Bar Area	0
Weight (lb)	0
Concrete Type	High-strength Concrete
Modulus of Elasticity (E_c)	105,000 ksi
Type of Span	one-way
Moment of Inertia (I_g)	3.04 in ⁴
Moment of Inertia (I_{cr})	10.71 in ⁴
Ultimate Flexure Capacity	6.87 in
Maximum Moment (M_{max})	188.84 in-kip
Cracking Moment (M_{cr})	60.7 in-kip
Cracking Due to Flexure	Yes
Maximum Strain (ϵ_{max})	0.0020
Available Concrete Strength (ksi) (Concrete M_{cr})	888 ksi
Failure Mode (yes/no)	shear
Flexure Shear Strength of Concrete (V_{cr})	0.000 kip
Failure Probability (Shear)	0.0000
Maximum Moment (M_{max})	171.12 in-kip
Cracking Moment (M_{cr})	8880 in-kip
Cracking Due to Flexure	Yes
Maximum Shear (V_{max})	171.09 kip
Overhead Shear Length of Concrete (V_{cr})	2000 kip
Failure Probability (Shear)	0.0000
Flexure Shear Strength of Concrete (V_{cr})	0.0000 kip
Failure Mode (yes/no)	flexure

Figure C-9: Blow-through analysis for scenario 6 for case study #2.

Depth to Top Reinforcing Bar (D_t)	1.0 ft
Effective depth (D_e)	5
Deck Thickness	6.5 ft
Depth to Bottom Reinforcing Bar	7 ft
Depth of Parapet to Bottom	9.175 ft
Number of Top Chords	1
Width of Pier	1
Number of Piers per	1
Hourly Diameter	1
Hourly Diameter	1
Angle of Load on	90
Plate Length (L_p)	1
Design Compressive Strength of Concrete	4
Design Tensile and Normal Strength	1
Design Normal Strength of Member	1
Compressive Strength of Top Chord Member ($\phi_c P_n$)	1
Length (L)	1
Height (H)	1
Effective Length	1
Appropriate Modifier	1
Grade of Steel (F_y)	400 MPa
Type of Span	one-way
Moment of Inertia (I_g)	4.08 m ⁴
Plastic Modulus (Z_p)	12.81 m ³
Design Section Modulus (Z_x)	1.16 m ³
Mass of Member (M_{self})	103.91 kN-m
Condition Mod. and C_p	0.75 (see 6)
Cracking Design Moment	179.49 kN-m
Modular Ratio (n)	1
One-Way Shear Strength of Concrete (ϕV_c)	1,000 kN
Failure in One-Way Shear	1
Two-Way Shear Strength of Concrete (ϕV_c)	1,000 kN
Failure in Two-Way Shear	1
Design Moment (M_u)	129.79 kN-m
Cracking Moment (M_{cr})	1,000 kN-m
Cracking Check ($M_u < M_{cr}$)	1
Design Moment (M_u)	131.09 kN-m
One-Way Shear Strength of Concrete (ϕV_c)	1,000 kN
Failure in One-Way Shear	1
Design Moment (M_u)	1,000 kN-m
Failure in Punching Shear	1

Figure C-10: Blow-through analysis for scenario 7 for case study #2.

Concrete Top Reinforcement Moment (M_{top})	27.71
Reinforcing Steel Area	5
Deck Thickness	8.5
Concrete Bottom Reinforcing Moment	5.46
Deck of Concrete Slab Area	3.211
Number of Pier Panels	1
Width of Pier	1
Deck Pier Distance	21
Deck Elevation	1
Angle of Load (1)	149
Point Load (1)	1
Design Compressive Strength (f_{cd})	64
Spring Deflection (Δ_{spring})	0.000
Average Strain at Failure of Concrete	0.002
Concrete strength based on 12 inch diameter Cylinder (1)	69
Concrete (1)	1
Concrete (2)	1
Concrete (3)	1
Concrete Type	1
Aggregate (Pulverized)	1
Number of Piers (1)	4.014
Type of Span	1
Minimum Reinforcement	1.45
Moment Inertia (I_g)	31.73
Distance to Neutral Axis (1)	0.101
Maximum Moment (M_{max})	283.54
Design Moment (M_d)	102.16
Deck of Deck Thickness	1
Masonry Shear ($V_{masonry}$)	191.19
Concrete Shear Strength of Concrete (V_c)	18.04
Failure of Concrete Shear	1
Reinforcing Steel Strength of Concrete (V_s)	1700
Concrete Pier Height (1)	1
Moment Inertia ($I_{p,1}$)	291.13
Deck of Pier (1)	1
Decking Height (1)	1
Masonry Shear ($V_{masonry}$)	181.47
Concrete Shear Strength of Concrete (V_c)	18.04
Failure of Concrete Shear	1
Reinforcing Steel Strength of Concrete (V_s)	1700
Failure of Reinforcing Steel	1

Figure C-11: Blow-through analysis for scenario 8 for case study #2.

APPENDIX D CHLORIDE CONCENTRATION AT TOP MAT OF REINFORCING STEEL WITH AN APPLIED SURFACE TREATMENT

Figures D-1, D-2, and D-3 show the numerical modeling results for the top mat of reinforcing steel in a concrete bridge deck with a 2.0-, 2.5-, or 3.0-in. OCD, respectively, with an applied surface treatment.

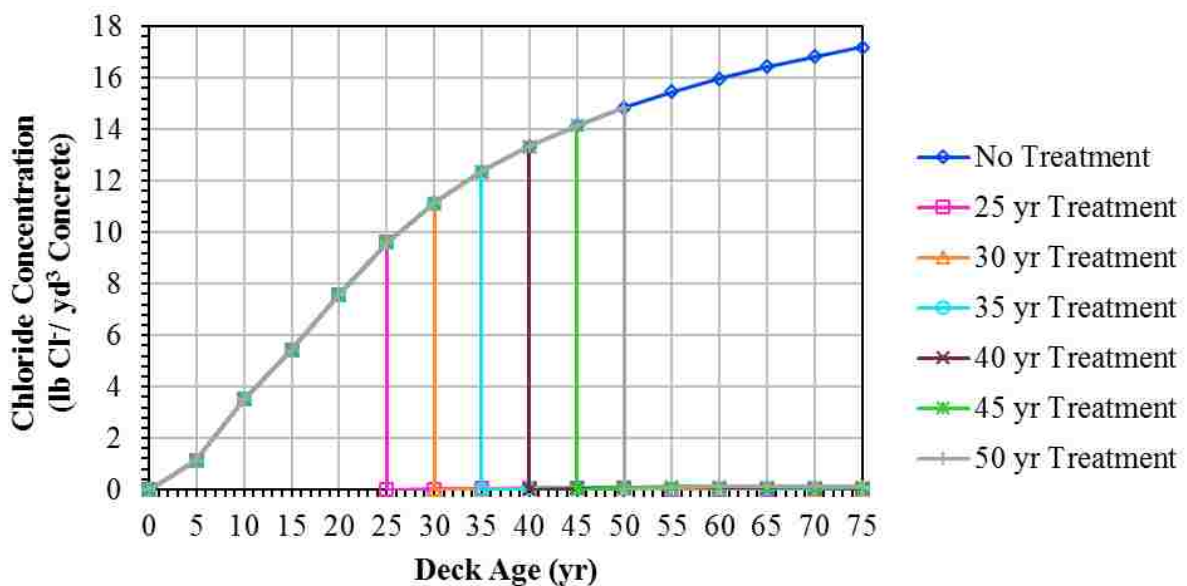


Figure D-1: Simulated chloride concentrations at the top mat of reinforcement for a deck with 2.0-in. OCD and a 3.375-in. removal depth with an applied surface treatment.

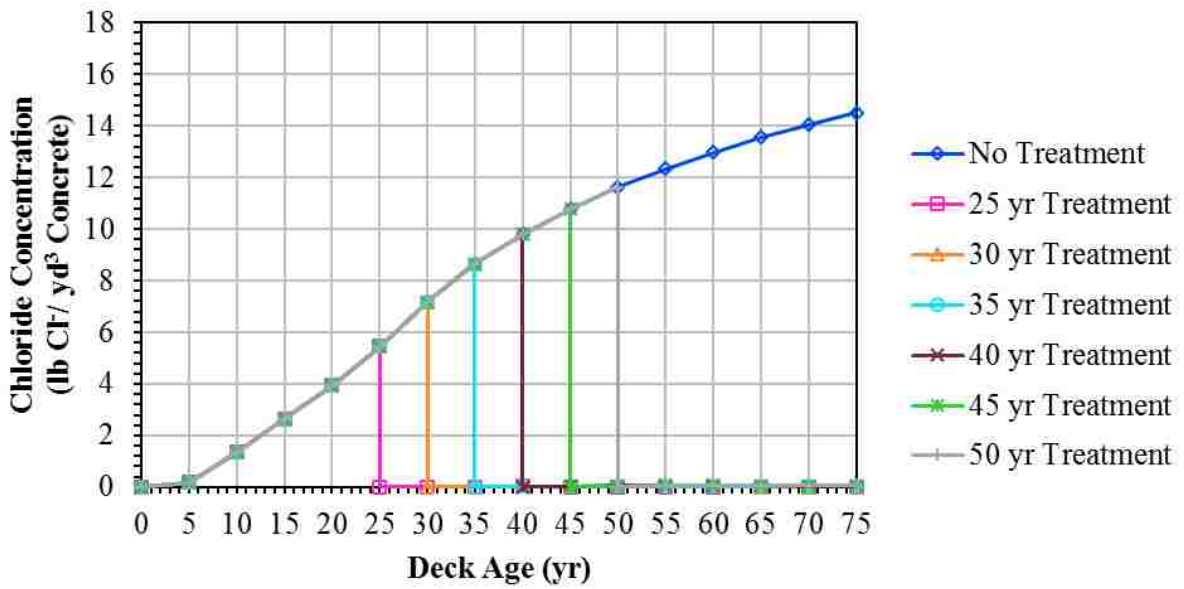


Figure D-2: Simulated chloride concentrations at the top mat of reinforcement for a deck with 2.5-in. OCD and a 3.875-in. removal depth with an applied surface treatment.

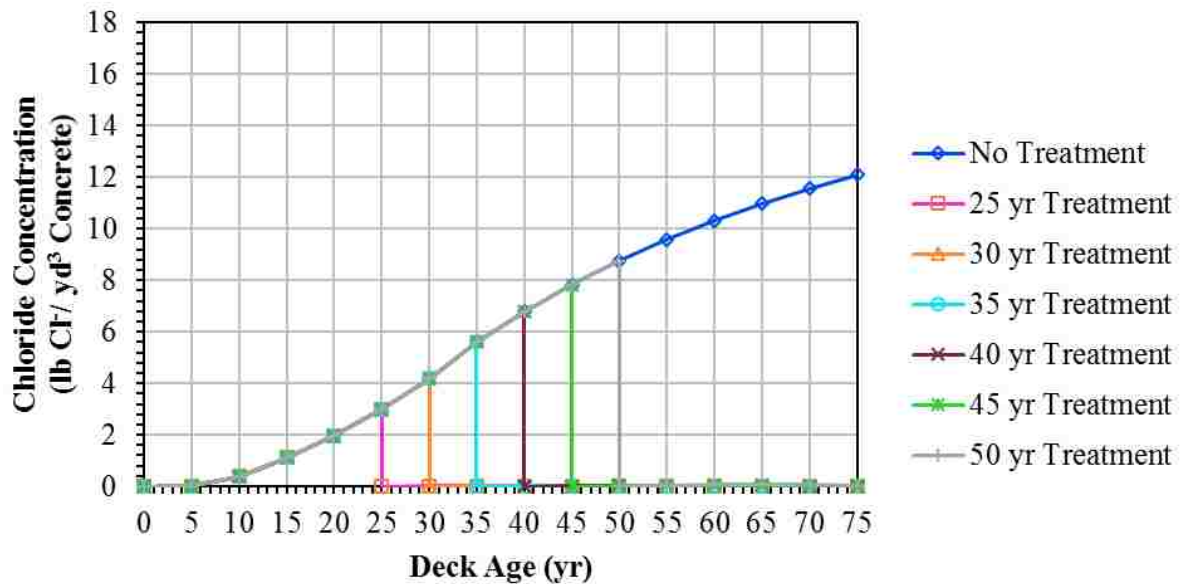


Figure D-3: Simulated chloride concentrations at the top mat of reinforcement for a deck with 3.0-in. OCD and a 4.375-in. removal depth with an applied surface treatment.

APPENDIX E CHLORIDE CONCENTRATION AT BOTTOM MAT OF REINFORCING STEEL WITH AN APPLIED SURFACE TREATMENT

Figures E-1, E-2, and E-3 show the numerical modeling results for the bottom mat of reinforcing steel in a concrete bridge deck with a 2.0-, 2.5-, or 3.0-in. OCD, respectively, with an applied surface treatment.

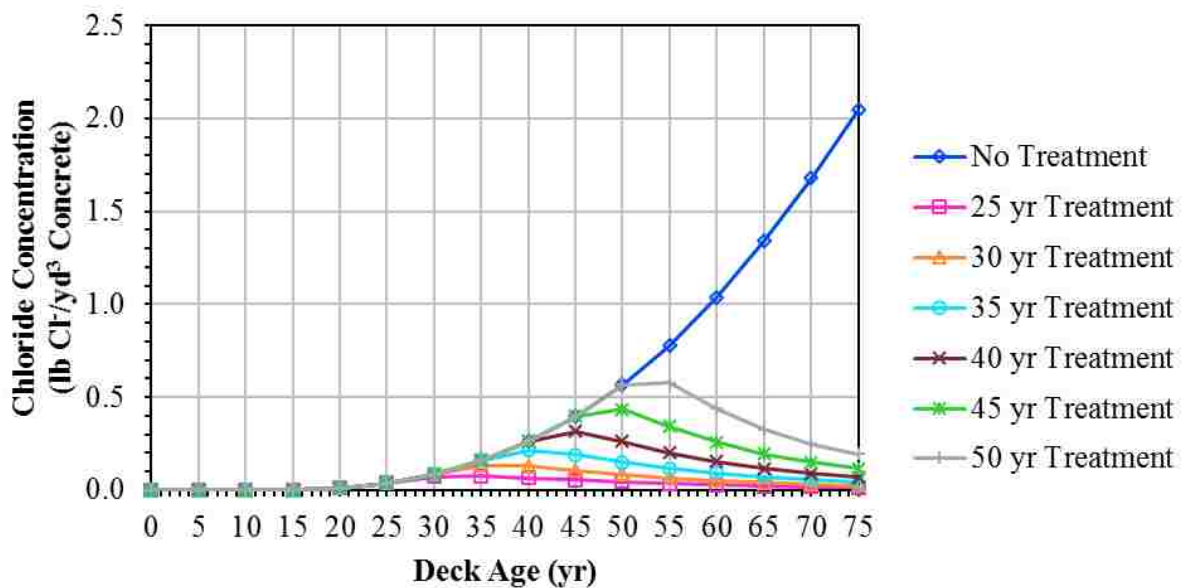


Figure E-1: Simulated chloride concentrations at the bottom mat of reinforcement for a deck with 2.0-in. OCD and a 3.375-in. removal depth with an applied surface treatment.

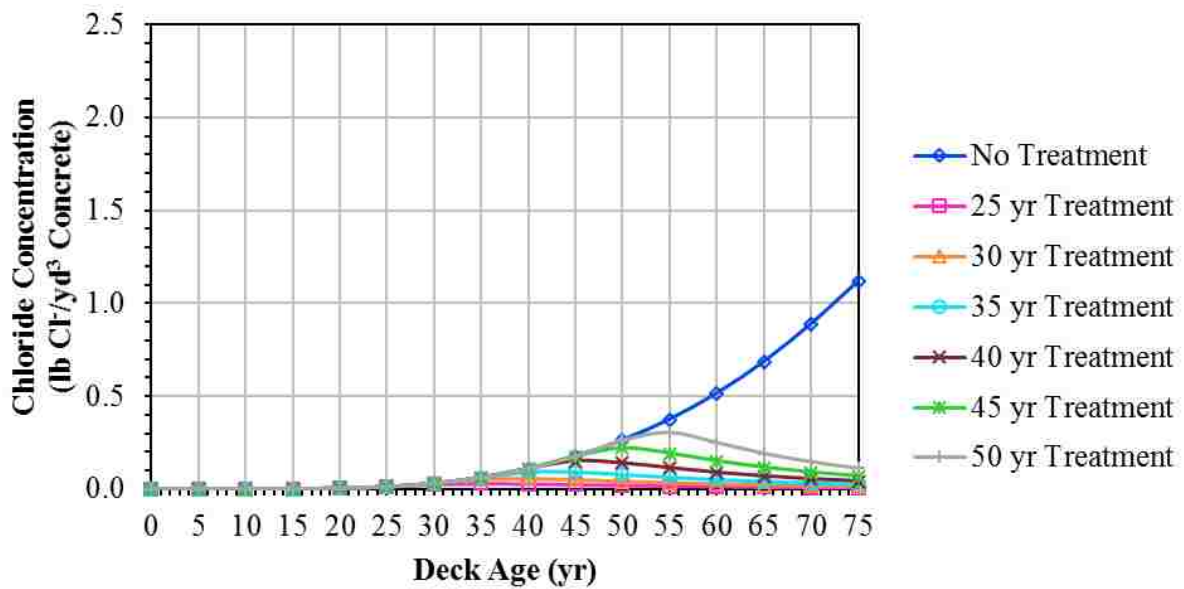


Figure E-2: Simulated chloride concentrations at the bottom mat of reinforcement for a deck with 2.5-in. OCD and a 3.875-in. removal depth with an applied surface treatment.

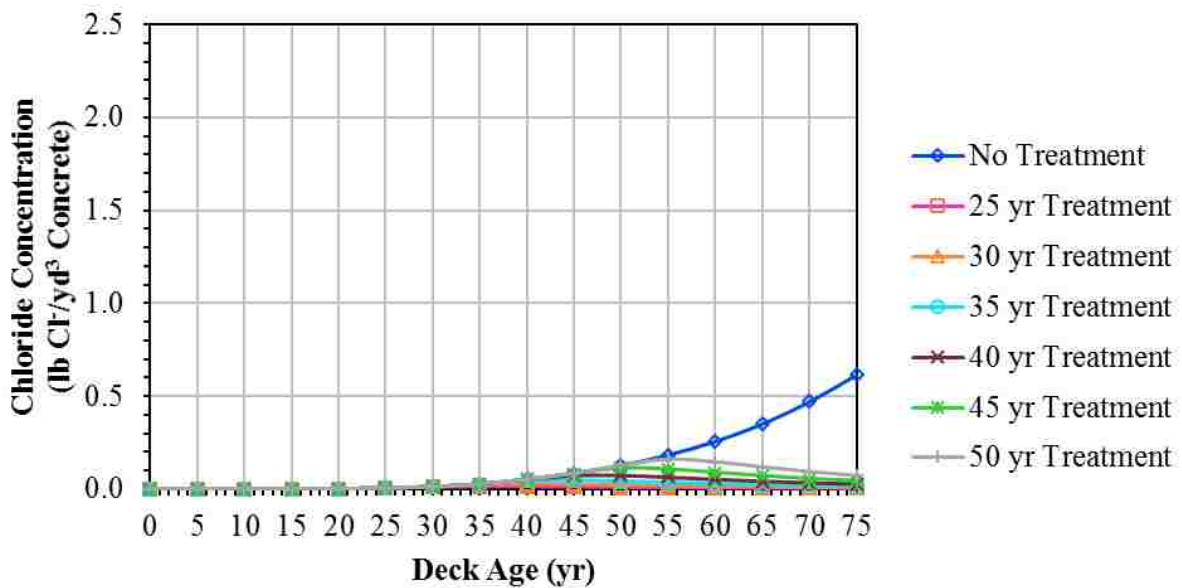


Figure E-3: Simulated chloride concentrations at the bottom mat of reinforcement for a deck with 3.0-in. OCD and a 4.375-in. removal depth with an applied surface treatment.

APPENDIX F CHLORIDE CONCENTRATION AT TOP MAT OF REINFORCING STEEL WITHOUT AN APPLIED SURFACE TREATMENT

Figures F-1, F-2, and F-3 show the numerical modeling results for the top mat of reinforcing steel in a concrete bridge deck with a 2.0-, 2.5-, or 3.0-in. OCD, respectively, without an applied surface treatment.

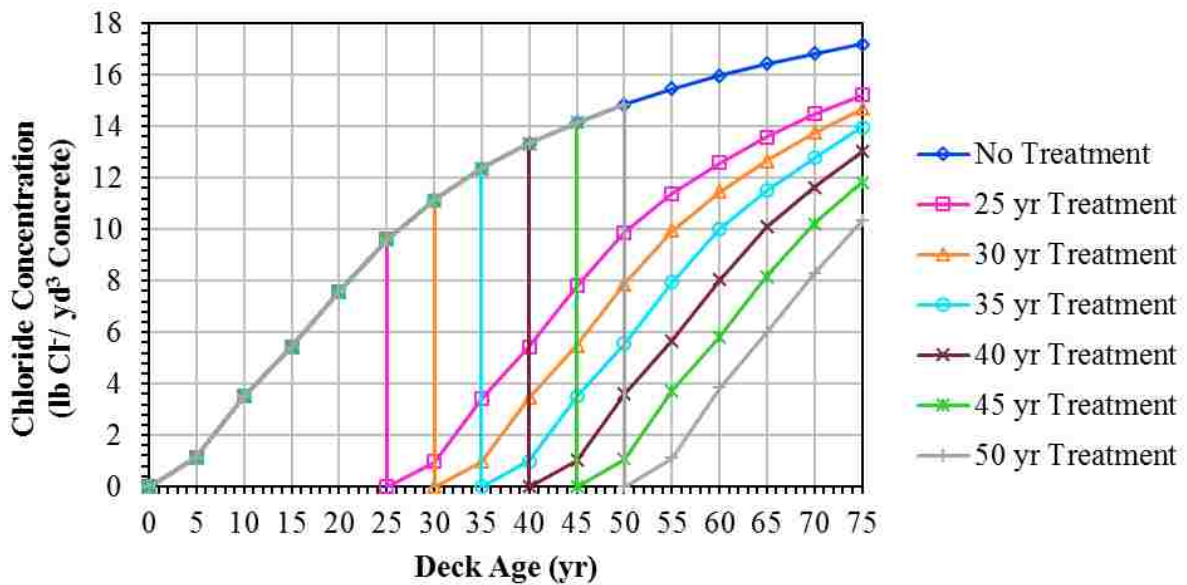


Figure F-1: Simulated chloride concentrations at the top mat of reinforcement for a deck with 2.0-in. OCD and a 3.375-in. removal depth without an applied surface treatment.

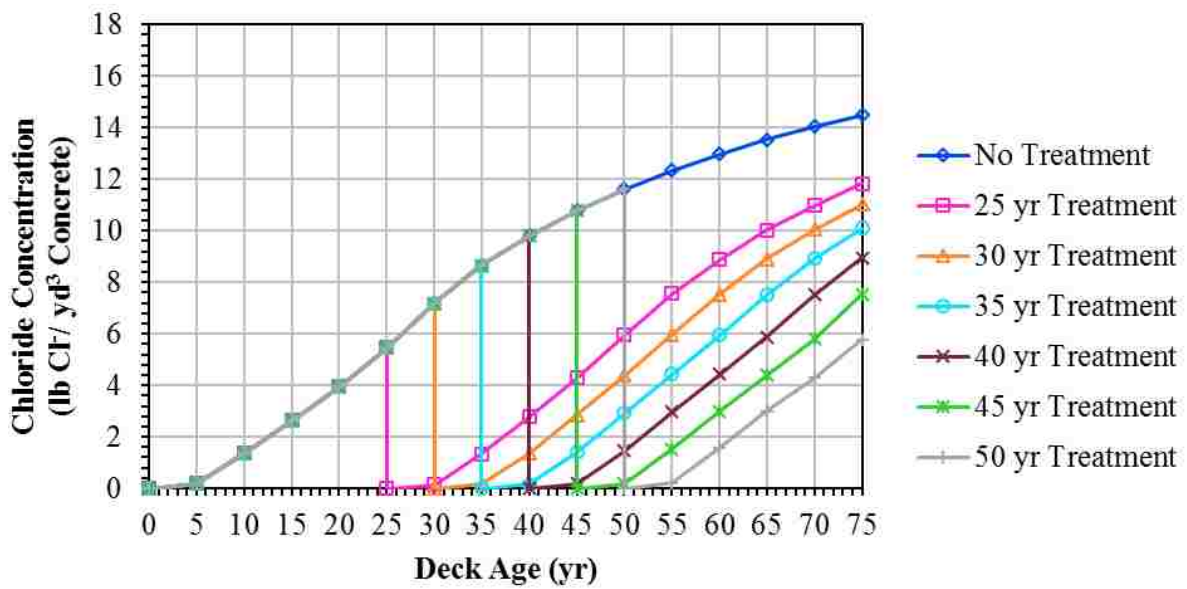


Figure F-2: Simulated chloride concentrations at the top mat of reinforcement for a deck with 2.5-in. OCD and a 3.875-in. removal depth without an applied surface treatment.

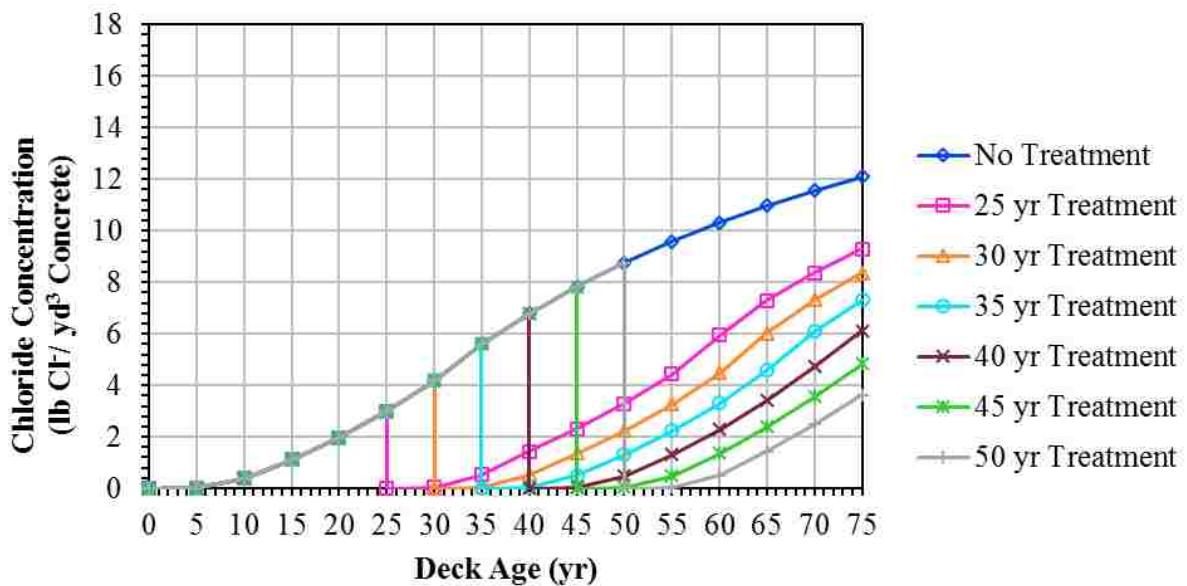


Figure F-3: Simulated chloride concentrations at the top mat of reinforcement for a deck with 3.0-in. OCD and a 4.375-in. removal depth without an applied surface treatment.

APPENDIX G CHLORIDE CONCENTRATION AT BOTTOM MAT OF REINFORCING STEEL WITHOUT AN APPLIED SURFACE TREATMENT

Figures G-1, G-2, and G-3 show the numerical modeling results for the bottom mat of reinforcing steel in a concrete bridge deck with a 2.0-, 2.5-, or 3.0-in. OCD, respectively, without an applied surface treatment.

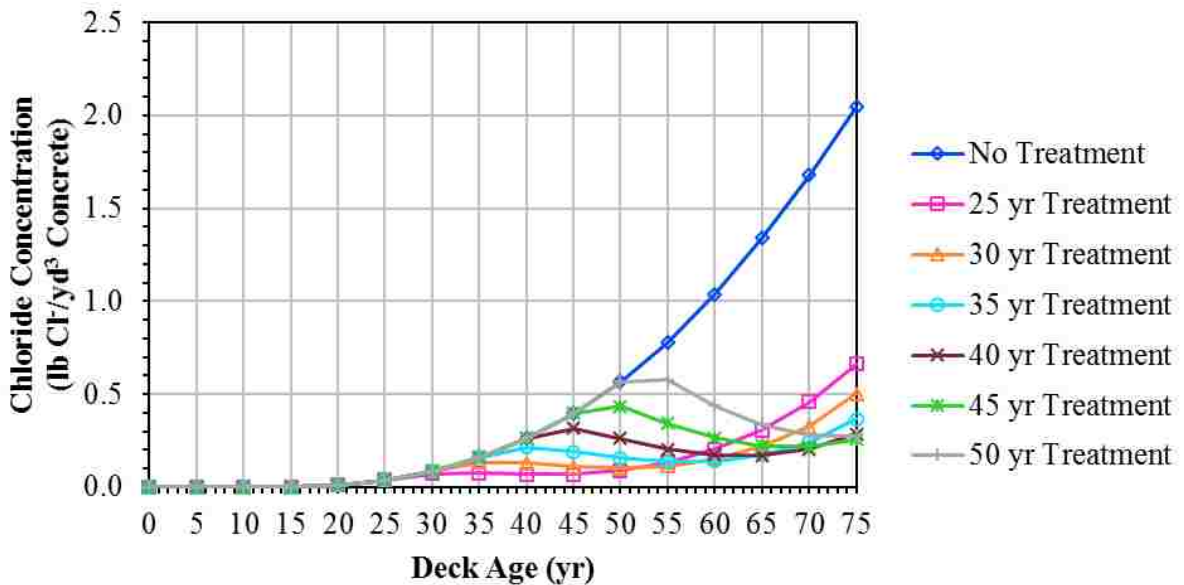


Figure G-1: Simulated chloride concentrations at the bottom mat of reinforcement for a deck with 2.0-in. OCD and a 3.375-in. removal depth without an applied surface treatment.

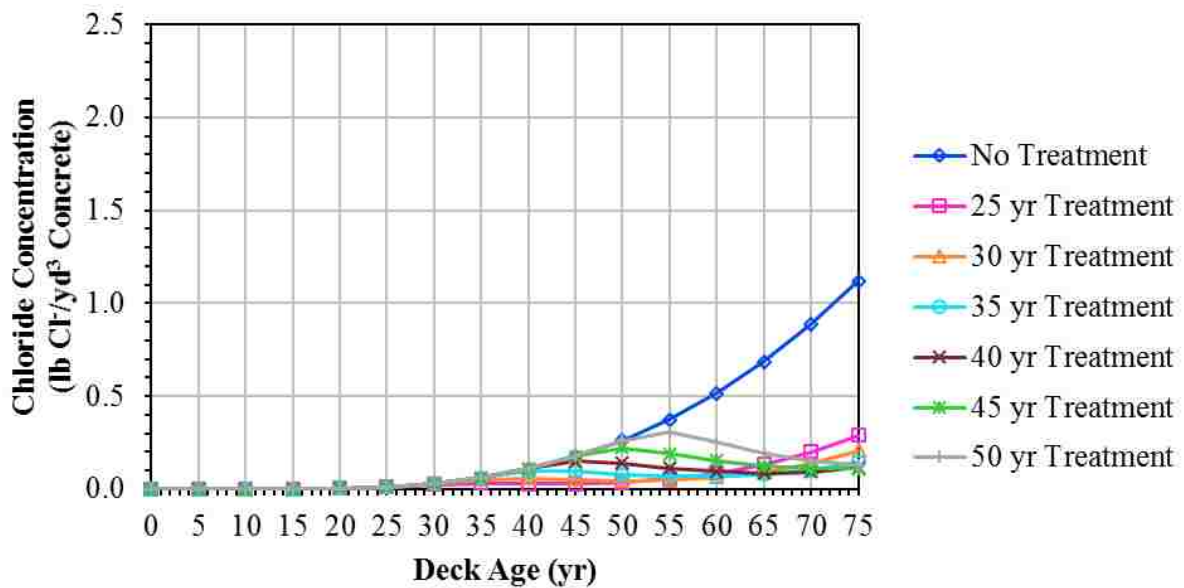


Figure G-2: Simulated chloride concentrations at the bottom mat of reinforcement for a deck with 2.5-in. OCD and a 3.875-in. removal depth without an applied surface treatment.

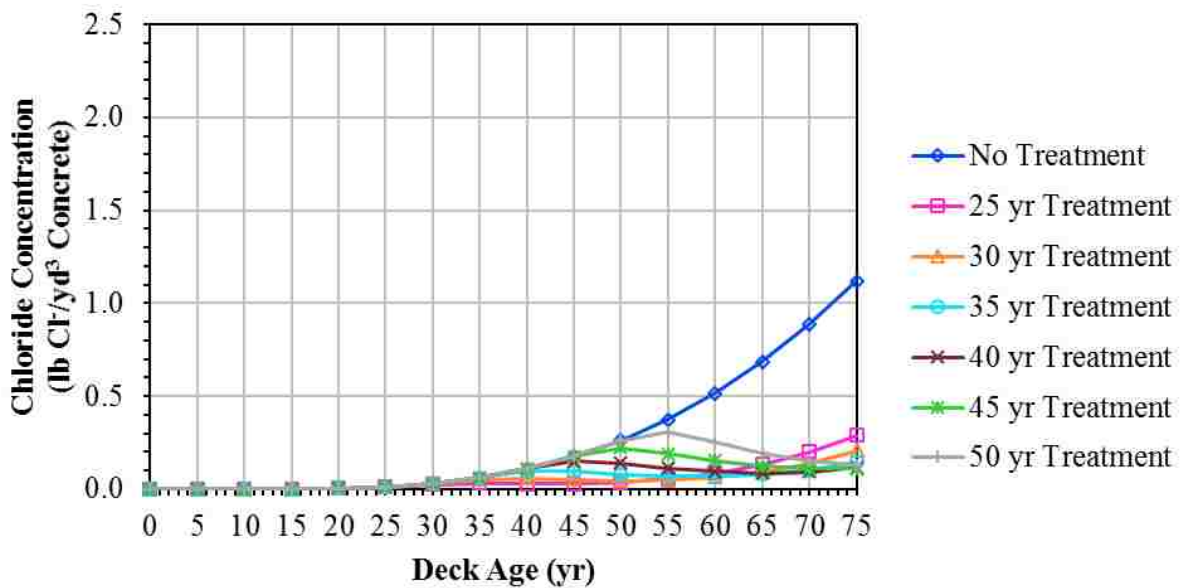


Figure G-3: Simulated chloride concentrations at the bottom mat of reinforcement for a deck with 3.0-in. OCD and a 4.375-in. removal depth without an applied surface treatment.